OPEN ACCESS
IOP Publishing | London Mathematical Society
Made open access 23 March 2020
Nonlinearity
Nonlinearity **32** (2019) 2667–2693
https://doi.org/10.1088/1361-6544/ab0b1d

Beyond all order asymptotics for homoclinic snaking in a Schnakenberg system

Hannes de Witt

Institut für Mathematik, Carl von Ossietzky Universität Oldenburg, D26111 Oldenburg, Germany

E-mail: hannes.de.witt@uni-oldenburg.de

Received 15 October 2018, revised 4 February 2019
Accepted for publication 27 February 2019
Published 18 June 2019

Recommended by Professor Guido Schneider

Abstract

Using multi-scale beyond all order methods, we investigate stationary spatially localized solutions of a Schnakenberg system, a prototype reaction–diffusion system, near the onset of a subcritical Turing bifurcation. These solutions are homoclinic orbits to a homogeneous solution and passing near a periodic solution. In bifurcation diagrams, branches of these solutions commonly show two interwining snaking curves. Here we calculate the maximal range of existence for these solutions and compare our findings with numerical computations. We derive and optimally truncate a (divergent) asymptotic series of a front solution. The remainder of the truncated series is exponentially small if and only if a specific parameter range is met. This complements work on Swift–Hohenberg equations where similar results have been obtained.

Keywords: snaking, pinning, localized pattern, beyond all orders, bifurcation
Mathematics Subject Classification numbers: 35J60, 35B32, 35B36, 35C20

(Some figures may appear in colour only in the online journal)

1. Introduction

Homoclinic snaking refers to the existence of a continuum of localized stationary solutions, homoclinic orbits to a homogeneous solution and passing near a periodic solution, in a parametrized partial differential equation, which commonly forms a snaking structure in bifurcation diagrams. This has been investigated in a variety of theoretical and experimental contexts, see e.g. [Daw10, Des11, Kno15, Kno08] for overviews and e.g. [MYG07, RAB+13] for some

concrete examples. An equation which is often used as a generic model for homoclinic snaking is the Swift Hohenberg equation:

$$\partial_t u = \lambda u - (1+\Delta)^2 u + N(u,\sigma) \tag{1}$$

with $u = u(x,t) \in \mathbb{R}, x \in \mathbb{R}$, and parameters $\lambda, \sigma \in \mathbb{R}$. Typical choices for the nonlinearity N are $f(u) = \sigma u^2 - u^3$ and $g(u) = \sigma u^3 - u^5$. The trivial solution $u \equiv 0$ loses stability at $\lambda_c = 0$ and for $\sigma > \sigma_0 \geqslant 0$ with $\sigma_0 = \sqrt{27/38}$ for $N = f$ and $\sigma_0 = 0$ for $N = g$ a periodic solution with wavenumber 1 bifurcates subcritically. In [CK09], equation (1) with nonlinearity f is analyzed with beyond all order methods to compute the existence range for localized patterns near the onset of the subcritical Turing bifurcation, and it is shown that the existence range is exponentially small in parameter space. The work in [CK09] is extended in [DMCK11], where the same method is used to investigate (1) with the nonlinearity g, and λ as the bifurcation parameter. In detail, constants μ and ν are derived such that

$$|\lambda - \lambda_{\mathrm{M}}| < \frac{\mu}{\sigma} \mathrm{e}^{-\frac{\nu}{\sigma}} \text{ if } 0 < \sigma \ll 1 \tag{2}$$

describes the existence range in λ, where λ_{M} is the so called Maxwell point. The constant ν is calculated analytically while μ is computed numerically only, but it is shown that μ is the limit of a recursive series. To achieve (2), an asymptotic expansion is derived by a multi-scale ansatz. Even though the calculation of the whole expansion and an estimate for the remainder is necessary to justify (2), it turns out that the result can essentially be computed with the knowledge of the leading order solution only. In detail, the pattern wavenumber and the behavior of the amplitude singularities closest to the real line determine ν up to an integer constant, which incorporates the lowest order nonlinearity, see also [KC13]. This indicates that beyond all order methods can be a strong tool to calculate snaking widths as the results can be established quite easy at least in the one dimensional case, even though the justification needs heavy computation.

The aim of this paper is to transfer the results of [CK09] and [DMCK11] to the Schnakenberg system

$$\partial_t U = D\Delta U + N(U,\lambda,\sigma), \quad N(U,\lambda,\sigma) = \begin{pmatrix} -u+u^2 v \\ \lambda - u^2 v \end{pmatrix} + \sigma \left(u - \frac{1}{v}\right)^2 \begin{pmatrix} 1 \\ -1 \end{pmatrix} \tag{3}$$

with $U = (u, v)(t,x) \in \mathbb{R}^2$, $x \in \mathbb{R}$ and diffusion matrix $D = \begin{pmatrix} 1 & 0 \\ 0 & d \end{pmatrix}$. The original Schnakenberg model [Sch79] ($\sigma = 0$) is widely used to understand the distribution of a morphogen, see, e.g. [GT85]. It was investigated for Turing pattern in 2D–3D, and recently [UW14] also investigated localized patterns in 2D not only on a homogeneous background, but also localized hexagon pattern on a background of stripes. In [UW14] the modification ($\sigma \neq 0$) was made to allow localized patterns between a homogeneous solution and stripes, and thus localized patterns in 1D.

We are interested in localized steady patterns, i.e. we aim for localized solutions of the equation

$$0 = D\Delta U + N(U,\lambda,\sigma). \tag{4}$$

The homogeneous solution $U^h \equiv \left(\lambda, \frac{1}{\lambda}\right)^T$ loses stability at $\lambda \leqslant \lambda_c = \sqrt{d}\sqrt{3-\sqrt{8}}$ and a periodic solution with wavelength $2\pi/k_c, k_c = \sqrt{\sqrt{2}-1}$ bifurcates subcritically for $\sigma_l < \sigma < \sigma_r < 0$ with $\sigma_r \approx -2.4 d^{-\frac{1}{2}}$ and $\sigma_l \approx -16 d^{-\frac{1}{2}}$. The exact values for σ_r and σ_l are computed, but omitted, as they are lengthy, see remark 2.3. We restrict ourself to $d > d_0$ with

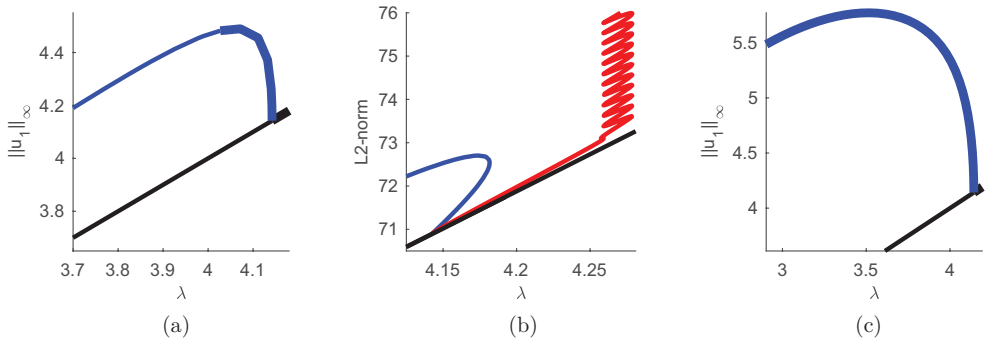

Figure 1. Homogeneous branch (black), periodic branch with wavelength $\frac{2\pi}{k_c}$ (blue), and in (b) a branch of localized patterns (red). The solutions are computed on the domain $\left(-\frac{15\pi}{k_c}, \frac{15\pi}{k_c}\right)$ with Neumann boundary conditions. (Numerically) stable branches as thick lines in (a), (b), while stability is not plotted in (b) to achieve better visualization and as we do not concern about the stability in the whole calculus. (a) $\sigma = -2$. (b) $\sigma = -1$. (c) $\sigma = 0$.

$d_0 = 3 + \sqrt{8}$, which is the condition for Turing instabilities at the homogeneous solution U^h. Figure 1 shows bifurcation diagrams for (3) for different values of σ, including a snaking branch of localized patterns.

Under the numerically confirmed assumption that localized patterns exist, we show that near σ_r and σ_l there is at most an exponentially small (in σ) λ-range, in which this localized patterns can exist. A numerical comparison will show that our formula approximates the exact range for localized pattern for σ close to σ_r and σ_l, respectively.

The calculations needed for this result are cumbersome, but in many parts similar to those in [CK09] and [DMCK11]. In contrast to [CK09] and [DMCK11] we investigate a two component system of reaction–diffusion type, which is non-variational and where the available numerical and analytical information is limited. The non-variational nature of the system does not have effects on the calculus itself, as non-variational effects are of smaller scale, but the definition of objects like the Maxwell point, in a variational system the point where the energy of both investigated solutions is the same, is less intuitive and requires the derivation of amplitude equations. The system case however complicates the analysis a lot, as e.g. the nonlinearities need to be understood as k-linear forms now and tend to have a complicate structure. We cope with these problems by calculating in a quite universal fashion, i.e. mostly treat the nonlinearities as arbitrary k-linear forms. This allows one to understand our calculation as a generalizations of these from [CK09] and [DMCK11]. We do not give general criteria for the calculation of ranges of localized patterns in arbitrary systems, but we have set up a Matlab symbolic toolbox script for the crucial computations, which can be adapted for arbitrary two component systems in a few steps. We also give a theorem-proof scheme, which supports further investigations of localized patterns in general systems.

The paper is organized as follows. In section 2 we state our main result, linearize the system around the homogeneous solution U^h and introduce some notations along with a new parameter ε in which we scale the equation. Then we derive the leading order front solution in an amplitude equation of order five in section 3 as the starting point for the beyond all order methods. In section 4 we construct the snaking width formula through beyond all order asymptotics, and in section 5 we give a set of equations for the snaking bifurcation diagram. In section 6 we compute the analytically undetermined constant μ numerically and compare

the findings with numerical computations of the model on a large, but finite domain, using pde2path [URW14].

2. Main result and first steps into the analysis

We investigate localized patterns at the onset of the subcritical bifurcation with wavelength $2\pi/k_c$. Lemma 2.1 describes this bifurcation, which is of particular interest, as the homogeneous solution loses stability here.

Lemma 2.1. *Let $d > 3+\sqrt{8}$. The trivial stationary solution $\left(\lambda, \frac{1}{\lambda}\right)^T$ of (3) is stable for $\lambda > \lambda_c = \sqrt{d}\sqrt{3-\sqrt{8}}$ and at $\lambda = \lambda_c$ a Turing instability occurs. The critical wavenumber is $k_c = \sqrt{\sqrt{2}-1}$.*

Proof. Calculus, following e.g. [Mur89, section 14.3]. □

It is such a Turing instability where fronts and localized patterns are expected, and by the introduction of a new parameter ε we make the ansatz

$$U_{\text{asymp}}(x,X) = \left(\lambda, \frac{1}{\lambda}\right)^T + \sum_{n=1}^{N} \varepsilon^n U_n(x,X) + R_N(x,X), \tag{5}$$

where $X = \varepsilon^2 x$ is a slow scale, to expand possible fronts in an asymptotic manner. This ansatz leads to amplitude equations, and to allow leading order front solutions a solvability condition for the amplitude of U_1 must not rise before $O(\varepsilon^5)$. This forces the scaling $\sigma = \sigma_0 + \varepsilon^2\sigma_2$, where two values ($\sigma_r$ and σ_l) for σ_0 are valid and describe the minimal resp. maximal σ for which a subcritical bifurcation and thus snaking can be observed. W.l.o.g. one can restrict $\sigma_2 \in \{-1, 1\}$, which we use for our hypothesis 2.2, while we keep σ_2 arbitrary in most calculations to track the σ dependence.

Our method, to expand the fronts with (5), does not give rigorous proof for the existence of these, as the remainder can not be uniformly controlled in higher orders, and thus we formally assume the existence of fronts in advance in hypothesis 2.2. The validity of hypothesis 2.2 is convincingly supported by numerical investigations.

Hypothesis 2.2 (Existence of stationary fronts). For $d > d_0$ and $(\sigma_0, \sigma_2) = (\sigma_r, -1)$, $\sigma_r \approx -2.4d^{-\frac{1}{2}}$ (case 1) respectively $(\sigma_0, \sigma_2) = (\sigma_l, 1)$, $\sigma_l \approx -16d^{-\frac{1}{2}}$ (case 2) there exist $\varepsilon_0 > 0$ and $\lambda_M(\varepsilon), k_M(\varepsilon) \in C\left((0,\varepsilon_0), \mathbb{R}\right)$ with $\lim_{\varepsilon\to 0} k_M(\varepsilon) = k_c$ and $\lim_{\varepsilon\to 0} \lambda_M(\varepsilon) = \lambda_c$ such that the following holds:

$\forall \varepsilon \in (0,\varepsilon_0)\ \exists C_{\text{loc}} > 0\ \forall\, |\lambda - \lambda_M(\varepsilon)| < C_{\text{loc}}\ \exists!\ U_\varepsilon^f$ solution[1] of (3) with $\sigma = \sigma_0 + \varepsilon^2\sigma_2$ and with

1. $\lim_{x\to-\infty} U_\varepsilon^f(x) = U^h(x)$
2. $\lim_{x\to\infty} \left|U_\varepsilon^f(x) - U_\varepsilon^{\text{per}}(x)\right| = 0$, where $U_\varepsilon^{\text{per}}(x) = U^h(x) + \varepsilon U_1(x)$ with $\|U_1\|_\infty = O(1)$ and minimal period $2\pi/k_M(\varepsilon)$, i.e. $U_1(x + 2\pi/k_M(\varepsilon)) = U_1(x)$.

[1] Where uniqueness is modulo symmetries, i.e. reflection and translation, only.

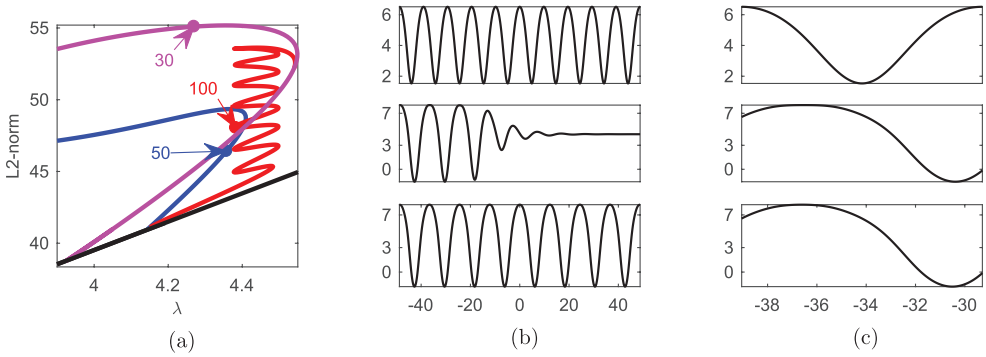

Figure 2. (a) Bifurcation diagram for $\sigma = -0.5$. The branch of localized patterns bifurcating from the periodic branch with wavelength $2\pi/k_c$ connects back to a periodic branch with wavelength $2\pi/0.515$. The precise wavelength depends on the domain of computation, and is highly inaccurate in this picture, as the domain size was reduced to $10 \cdot 2\pi/k_c$ to give a full view on the branch of localized patterns. The general phenomenon however is described by the analysis. (b), (c) Solutions on the periodic branches and the branch of localized patterns and a zoom on an interval of length $2\pi/k_c$. The difference in the period for point `100` and `30` is due to wavenumber variations inside the snake, see e.g. [BD12].

Remark 2.3.

1. σ_0 is computed exactly, but we only give approximate values, as the exact expressions are lengthy. If not stated otherwise, this holds for all constants and $\approx$ describes approximated values for notational reasons only. Calculations are always done with the exact values.
2. The point λ_M, describing the center of the range for localized patterns, is the non-variational analog of the Maxwell point in a variational system where the energy of the homogeneous and periodic solution is the same. It is determined via a series in ε, with coefficients that are determined by solvability conditions for amplitude equations for fronts, which we derive later.

The introduction of k_M rather than the constant wavenumber k_c is necessary because the amplitude of the front derived with (5) is complex and thus will shift the wavenumber by $O\left(\varepsilon^2\right)$. As a consequence we do not construct fronts which connect a periodic solution with wavenumber k_c with the homogeneous solution for $|\sigma - \sigma_0| > 0$. This is in accordance with the numerical simulations where the branch of localized patterns bifurcating from the periodic branch with wavenumber k_c immediately changes its periods and connects to the most sub-critical wavenumber, see figure 2. Also the wavenumber breathing within the snake, see e.g. [BD12], forces the introduction of k_M.

Theorem 2.4, which is a simplified version of the main result of this work, gives an upper bound for the constant C_{loc} near σ_l respectively σ_r.In section 4.4, theorem 4.5 we give the more precise version, which however needs the introduction of additional notations, and conclude its proof.

Theorem 2.4 (An upper bound for C_{loc}). *Under hypothesis 2.2 there exists an $0 < \varepsilon_1 \leqslant \varepsilon_0$ and constants $\mu, \nu > 0$ such that for $0 < \varepsilon < \varepsilon_1$ we have*

$$C_{loc} < \frac{\mu}{|\sigma - \sigma_0|} e^{-\frac{\nu}{|\sigma - \sigma_0|}},$$

where $\nu \approx 18.550 d^{-\frac{1}{2}}$ in case 1 and $\nu \approx 69.721 d^{-\frac{1}{2}}$ in case 2.

Remark 2.5.

1. $\nu = k_c\pi/\varepsilon^2 b_2(\sigma_2)$, where b_2 will be introduced in section 3 and scales the amplitudes speed. The formula for b_2 is (very) lengthy and thus omitted here. k_c is the critical wavenumber, π is model independent and a scalar factor, here 1, is determined by the power of the lowest order nonzero nonlinearity (quadratic or cubic).
2. μ can only be given as a limit of a recursive series with nested sums and thus has to be investigated numerically. For this, the recursion can be used, which is computationally expensive, see [DMCK11], or μ can be found by a best fit with the numerical snaking width, see section 6.

To derive theorem 2.4 we do not only need the proper scaling of $\sigma = \sigma_0 + \varepsilon^2\sigma_2$, but also a proper scaling for λ which is

$$\lambda = \lambda_c + \sum_{n=0}^{\lfloor \frac{N}{4} \rfloor} \varepsilon^{4n}\lambda_{4n} + \varepsilon^4\lambda_\delta = \lambda_{\mathrm{M}}(\varepsilon) + \varepsilon^4\lambda_\delta, \tag{6}$$

where $\lambda_{4s}, s \in \mathbb{N}$ will be determined by the calculus and we will show that λ_δ can be chosen arbitrarily in a certain range. This range will then describe the constant C_{loc}. For the further calculus, i.e. the proof of theorem 2.4, we expand (4) at the homogeneous solution, so that for solutions $U^h + U$ (4) takes the form

$$0 = L[\Delta, \lambda]U + \sum_{k=2}^{\infty} F^k[\lambda, \sigma](U^k),$$

where $L[\Delta, \lambda] = J(\lambda) + D\Delta$ with $J(\lambda) = \begin{pmatrix} 1 & \lambda^2 \\ -2 & -\lambda^2 \end{pmatrix}$ and $F^k(U^k)$, $U^k = (U, \ldots, U)$, are k-linear forms. With the scaling $\lambda = \lambda_c + \varepsilon^4\lambda_4 + \ldots$ and $\sigma = \sigma_0 + \varepsilon^2\sigma_2$ these forms have a natural expansion in ε, namely

$$F_j^k[\lambda, \sigma](U^k) = F_0^k[\lambda_c, \sigma_0](U^k) + \varepsilon^2 F_2^k[\lambda_c, \sigma_2](U^k) + \varepsilon^4 F_4^k[\lambda_c, \lambda_4](U^k) + \cdots = \sum_{j \in 2\mathbb{N}_0} \varepsilon^j F_j^k[\lambda, \sigma](U^k).$$

This notation let us reformulate the expansion of (4) at the homogeneous solution and, by $\Lambda = \partial_x^2 + 2\varepsilon^2\partial_x\partial_X + \varepsilon^4\partial_X^2$, as $U = U(x, X(x))$, we have

$$\begin{aligned} 0 = &\left(L_0[\partial_x, \lambda_c] + \varepsilon^2 L_2[\partial_x, \partial_X, \lambda_c] + \varepsilon^4 L_4[\partial_X, \lambda_c, \lambda_4] + \varepsilon^4(\partial_\lambda J)(\lambda_c)\lambda_\delta + O\left(\varepsilon^8\right)\right) U \\ &+ \sum_{j \in \{0,2\}} \sum_{k=2}^{5-j} \varepsilon^j F_j^k[\lambda, \sigma_j](U^k) + \ldots, \end{aligned} \tag{7}$$

where $L_0[\partial_x, \lambda_c] = J(\lambda_c) + \partial_x^2 D, L_2[\partial_x, \partial_X, \lambda_c] = 2\partial_x\partial_X D$ and $L_4[\partial_X, \lambda_c, \lambda_4] = (\partial_\lambda J)(\lambda_c)\lambda_4 + \partial_X^2 D$.

The $O\left(\varepsilon^8\right)$ terms are from the expansion of the linear part L by the scaling of λ, the … are higher order nonlinearities respectively higher order expansion of the nonlinearities in σ and will be $O(\varepsilon^6)$ in the subsequent computations, as ansatz (5) scales every non homogeneous addend with factor ε. They both play no role in the subsequent calculations. For this reason it is the system without the higher order nonlinearities, which we investigate in section 6, and call it the 'truncated system'. The calculations are valid for both the full and the truncated

system, as the higher order nonlinearities are only incorporated in the constant μ, which we do not calculate analytically.

The further calculations to prove theorem 2.4 are structured by additional theorems. These aim to give an overview of the whole method rather than to depict every underlying result in detail. We end this section by the introduction of some abbreviations.

Definition 2.6. Some commonly used abbreviations are:

- $e_k = e_k(x) = \mathrm{e}^{\mathrm{i}k_c k(x+\omega)}$, where ω is a constant describing the phase shift and will be arbitrary until the control of the remainder of the asymptotic expansion.
- c.c. denotes the complex conjugated.
- h.o.t. is used in combination with asymptotic equivalents and denotes higher order terms in the corresponding variable.
- $a(x,z) \underset{x\to y}{\sim} b(x,z)$, where $(x,z) \in \mathbb{R}\times\Omega \subset \mathbb{R}\times\mathbb{C}^n$ and $y \in \mathbb{R}\cup\{-\infty,\infty\}$, is defined by
$$\forall \varepsilon > 0\ \forall z \in \Omega\ \exists \delta > 0 : |x-y| < \delta \Rightarrow |a(x,z) - b(x,z)| < \varepsilon$$
and the analog for $y \in \{-\infty,\infty\}$.
- Integration in the complex plane is always from a point X_0 on the imaginary axis to a point X on the real line, and the starting point is only chosen to have no constant terms. A possible path of integration is always the direct connection from X_0 to 0 to X and thus we only write $\int_{X_0}^{X} \mathrm{d}T$.

Furthermore, many constants are defined in the Theorems and their proofs. Some of these constants are necessary in later steps of the calculation, but as these can not be motivated before their introduction we refrain from a list here.

3. Amplitude equation

As stated in the introduction, the exponential factor in the snaking width can be expressed in terms of the leading order amplitudes complex singularities closest to the real line. We derive this leading order amplitude now and summarize the result in theorem 3.1. For clarity we only give the results for case 1 of hypothesis 2.2 here. The resulting constants for case 2 are given at the end of this section.

Theorem 3.1. *Let (5) be an asymptotic expansion of a front solution U_ε^f as in hypothesis 2.2 with λ scaled by (6). Then $\lambda_4 \approx 0.0042 d^{\frac{3}{2}}\sigma_2^2$ and*

$$U_1(x,X) = A(X)\Phi e_1(x) + \text{c.c.}$$

where $e_1(x) = \mathrm{e}^{\mathrm{i}k_c(x+\omega)}$ with an arbitrary constant ω, $\Phi = (1,\varphi_2)$ with $\varphi_2 \approx -3.414/d$, and

$$A(X) = R_0(X)\mathrm{e}^{\mathrm{i}\Theta_0(X)} = \frac{b_1 \mathrm{e}^{-b_2\frac{X}{2}}}{(1+\mathrm{e}^{-b_2 X})^{\frac{1}{2}+\mathrm{i}\beta}}$$

with constants $b_2 < 0 < b_1, \beta > 0$.

Proof. We insert ansatz (5) in (7) and sort for powers of ε. This yields

$$
\begin{aligned}
\varepsilon^1: &\quad -L_0U_1 = 0\\
\varepsilon^2: &\quad -L_0U_2 = F_0^2(U_1^2)\\
\varepsilon^3: &\quad -L_0U_3 = L_2U_1 + 2F_0^2(U_1,U_2) + F_0^3(U_1^3)\\
\varepsilon^4: &\quad -L_0U_4 = L_2U_2 + 2F_0^2(U_1,U_3) + F_0^2(U_2^2) + 3F_0^3(U_1^2,U_2) + F_0^4(U_1^4) + F_2^2(U_1^2)\\
\varepsilon^5: &\quad -L_0U_5 = L_2U_3 + L_4U_1 + 2F_0^2(U_1,U_4) + 2F_0^2(U_2,U_3)\\
&\qquad\qquad + 3F_0^3(U_1^2,U_3) + 3F_0^3(U_1,U_2^2) + 4F_0^4(U_1^3,U_2) + F_0^5(U_1^5)\\
&\qquad\qquad + F_2^3(U_1^3) + 2F_2^2(U_1,U_2).
\end{aligned}
\tag{8}
$$

...

The equations at $\varepsilon^k, k \leqslant 4$, can be solved without assumptions on the leading order amplitude. Via a solvability condition the equation at ε^5 results in the amplitude equation for the leading order solution. In detail the equation at $O(\varepsilon^1)$ yields

$$U_1 = A(X)\Phi e^{ik_0(x+\omega)} + \text{c.c.},$$

where $A(X)$ and ω are arbitrary for now while Φ and k_0 are determined by the equation

$$0 = \left(J(\lambda_c) - k_0^2 D\right)\Phi. \tag{9}$$

In the following we write x for $x+\omega$, as the phase shift does not influence most calculations. In the end we however have to reverse this notation, as it is a locking of the phase shift, which allows us to construct an (in leading order) exponentially small remainder for $\lambda_\delta \neq 0$, and thus ω is crucial for the calculation of the snaking width.

Following [Mur89, 14.3], as for the proof of lemma 2.1, there is a unique (up to a scalar factor) nontrivial solution for (9) if and only if $k_0 = \sqrt{\sqrt{2}-1} =: k_c$ and $\lambda_c = \sqrt{d}\sqrt{3-\sqrt{8}}$. We fix such a solution $\Phi \approx (1,\varphi_2)^T$ with $\varphi_2 \approx -3.414/d$ as the kernel vector.

The set of equation (8) yields $U_n = \sum_{k=-n}^{n} A_{n,k}\Phi_{n,k}e^{ikk_cx}$, where w.l.o.g. we assume $A_{n,k}(X)$ scalar and $\Phi_{n,k} \in \mathbb{C}^2$, see remark 3.2 for details. Of course $A_{1,1} = A$, $A_{1,-1} = \bar{A}$ and $\Phi_{1,1} = \Phi_{1,-1} = \Phi$ here. Furthermore, we introduce $L(s,\lambda_c) := J(\lambda_c) - s^2k_c^2D$ and see that $L(s,\lambda_c)$ has a nontrivial kernel for $s = 1$ only, as mentioned above. Thus it is invertible for $s \neq 1$, and by doing so one can calculate $A_{n,k}\Phi_{n,k}$ for $n \leqslant 4$ and $k \neq \pm 1$. For $k = \pm 1$ one has to ensure that the right hand side of the equations is orthogonal to the one dimensional kernel of $L(\pm 1,\lambda_c)$ i.e. that the solvability condition $\langle' \text{right hand side}', \Phi_\perp\rangle = 0$ for some $\Phi_\perp \in \text{Ker}(L(1,\lambda_c)^T)$ is met. At $\varepsilon^1, \varepsilon^2$ this is always satisfied, i.e. $A_{2,\pm 1}$ is arbitrary, but at ε^3 this is true if and only if

$$2F_0^2(\Phi,\Phi_{2,0}) + 2F_0^2(\bar{\Phi},\Phi_{2,2}) + 3F_0^3(\Phi^3) = 0. \tag{10}$$

This is the equation, which fixes $\sigma_0 \approx -2.4d^{-\frac{1}{2}}$ for case 1 and $\sigma_0 \approx -16d^{-\frac{1}{2}}$ for case 2. Fixing one case, the equation at ε^3 yields $A_{3,\pm 1}\Phi_{3,\pm 1} = i\partial_X A_{1,\pm 1}\tilde{\Phi}_{3,1} + A^{\Phi}_{3,\pm 1}\Phi$ with arbitrary $A^{\Phi}_{3,\pm 1}$. For the loose notation see remark 3.2. Here $A^{\Phi}_{3,\pm 1}\Phi$ can w.l.o.g. be set zero, as it does not contribute to any results. Also the equation for $A_{4,\pm 1}\Phi_{4,\pm 1}$ is solvable without additional restrictions and as the results are not relevant for the calculation of $A_{1,\pm 1}$ we will not discuss them here.

The solvability condition arises at $\varepsilon^5 e_{\pm 1}$ and results in an equation for A of the form

$$0 = c_0\partial_X^2 A + c_1 A + c_2|A|^2A + c_3|A|^4A + \mathrm{i}c_4A^2\partial_X\bar{A} + \mathrm{i}c_5|A|^2\partial_X A \tag{11}$$

with real constants $c_0(\sigma_0,\sigma_2,\lambda_4),\ldots,c_5(\sigma_0,\sigma_2,\lambda_4)$. The ansatz $A = R_0\mathrm{e}^{\mathrm{i}\Theta_0}$ with real functions R_0,Θ_0 splits this complex equation into two real ones where the equation for Θ_0

$$0 = 2c_0R_0\Theta_0' + c_0R_0\Theta_0'' + (c_5+c_4)R_0^2R_0' \tag{12}$$

has the particular solution of interest $\Theta' = \frac{c_5+c_4}{4c_0}R_0^2$, see remark 3.3. This yields

$$0 = c_0R_0'' + c_1R_0 + c_2R_0^3 + \left(c_3 - \frac{(c_5+c_4)^2}{16c_0} + \frac{c_5^2-c_4^2}{4c_0}\right)R_0^5, \tag{13}$$

as the equation for R_0.

As stated in theorem 3.1 we look for a front solution, i.e. a heteroclinic orbit from zero to a nonzero state. For this we investigate

$$E(R_0,R_0') = -\frac{c_0}{2}R_0'^2 + \frac{c_1}{2}R_0^2 + \frac{c_2}{4}R_0^4 + \frac{c_6}{6}R_0^6$$

with $c_6 = c_3 - \frac{(c_5+c_4)^2}{16c_0} + \frac{c_5^2-c_4^2}{4c_0}$, the energy of equation (13), i.e. solutions lie on the level set of E. As $E(0,0) = 0$ is a local maximum this implies that for the existence of localized patterns a maximum $(f,f') \neq (0,0)$ with $E(f,f') = 0$ must exist. This is the case if and only if $3c_2^2 - 16c_1c_6 = 0$ and $c_1,c_6 < 0 < c_2$. Furthermore, $\mathrm{sign}(c_2) = -\mathrm{sign}(\sigma_2)$ for case 1 and thus the condition $c_2 > 0$ implies $\sigma_2 < 0$, which is also the condition for the bifurcation to be subcritical. For fixed $\sigma_0 < 0$ all conditions are fulfilled if and only if $\lambda_4 = c_{\lambda_4}d^{\frac{3}{2}}\sigma_2^2$ with $c_{\lambda_4} \approx 0.0042$ and a front solution can be found via separation of variables. Such a solution combined with the solution for Θ_0, gives the full solution

$$A(X) = R_0(X)\mathrm{e}^{\mathrm{i}\Theta_0(X)} = \frac{b_1\mathrm{e}^{-b_2\frac{X}{2}}}{(1+\mathrm{e}^{-b_2X})^{\frac{1}{2}+\mathrm{i}\beta}},$$

with $b_1 \approx 0.148d^{\frac{3}{4}}\sqrt{|\sigma_2|}$, $b_2 \approx 0.109\sqrt{d}\sigma_2$ and $\beta \approx 0.119$. □

For case 2, i.e. $\sigma_0 \approx -15.894d^{-\frac{1}{2}}$, the corresponding constants are

$$b_1 \approx 0.0373d^{\frac{3}{4}}\sqrt{\sigma_2},\quad b_2 \approx 0.029\sqrt{d}\sigma_2,\quad \beta \approx -1.174,\quad \lambda_4 \approx 0.000\,29d^{\frac{3}{2}}\sigma_2^2$$

and $\sigma_2 > 0$ is the condition for the existence of a front.

Remark 3.2. It is $U_n = \sum_{k=-n}^{n} A_{n,k}\Phi_{n,k}\mathrm{e}^{\mathrm{i}kk_cx}$ with scalar $A_{n,k}(X)$ and $\Phi_{n,k} \in \mathbb{C}^2$ for $n \leqslant 2$ only, but for $n \geqslant 3$ we still can express the contribution of U_n at each e_k with a finite sum of scalar functions $A_{n,k}^j(X)$ and $\Phi_{n,k}^j \in \mathbb{C}^2$ and in further calculations one summand for each tuple (n,k) is crucial only, i.e. the others can w.l.o.g. be set to zero. Thus we stick to the loose but simpler notation $U_n = \sum_{k=-n}^{n} A_{n,k}\Phi_{n,k}\mathrm{e}^{\mathrm{i}kk_cx}$.

Remark 3.3. The solution for the homogeneous part of (12) is $\gamma\frac{1}{R_0'}$ with $\gamma\in\mathbb{R}$, but $\gamma\neq 0$ is in contradiction to $R_0(X)\to 0$ for either $X\to-\infty$ or $X\to\infty$.

4. Beyond all orders calculation

The leading order solution, established in section 3, gives a basic estimate for the form of localized patterns, but the existence range remains undetermined, even though λ_4 is fixed and gives a first approximation where localized patterns or more precisely the Maxwell point can be found. The calculation of further algebraic terms in the asymptotic expansion (5) yields higher order λ_{4s}, but is unable to determine an existence range.

In fact the series diverges and thus has to be truncated. To construct an uniformly exponentially small remainder, e.g. a remainder 'beyond all (algebraic) orders', the truncation has to be done optimally and certain conditions on λ_δ, the deviation from the Maxwell point, have to be met.

The error terms contributing to the remainder are the error by deviation from the Maxwell point λ_{M}, which is independent on the truncation point and thus denoted by R^{λ_δ}, and the error by truncation R_N^T. For the truncation error we need to calculate the behavior of U_n for $n\to\infty$, which we do next in section 4.1. In section 4.2 we calculate the error by the deviation of the Maxwell point and in section 4.3 the error by truncation. By the linearity of the asymptotic calculations the final remainder R_N can then be constructed as the sum of both remainders along with higher order terms, i.e. it is $R_N=R_N^T+R^{\lambda_\delta}+\text{h.o.t.}$. We will see, that R_N^T dominates for $X=O(\varepsilon)$, i.e. in the front's interface, and R^{λ_δ} dominates for $X\to\pm\infty$. The matching of both errors yields that the full remainder is uniformly exponentially small (in $\sigma-\sigma_0$) in leading order, if and only if $\varepsilon^4\lambda_\delta$, the deviation from λ_{M}, is exponentially small in $\sigma-\sigma_0$.

4.1. Behavior of the amplitude for n large

In section 3 we derived the exact form of U_1, see theorem 3.1. The next step is to derive the form of U_n for $n\to\infty$. In detail we prove the following theorem

Theorem 4.1. *Let (5) be an asymptotic expansion of a front solution U_ε^f as in hypothesis 2.2. Then*

$$\begin{aligned}U_n \underset{n\to\infty}{\sim} & p_1\left(\frac{\mathrm{e}^{\mathrm{i}\frac{\pi}{4}}}{\sqrt{k_c}}\right)^n\frac{\Gamma(\frac{n}{2}+\alpha)}{(X_0-X)^{\frac{n+1}{2}+\alpha}}(1+(-1)^n)\,(I_2(X)\Phi+I_1(X)\Phi e_2)\\ &+p_2\left(\frac{\mathrm{e}^{\mathrm{i}\frac{3\pi}{4}}}{\sqrt{k_c}}\right)^n\frac{\Gamma(\frac{n}{2}+\bar\alpha)}{(X_0-X)^{\frac{n+1}{2}+\bar\alpha}}(1+(-1)^n)\,(I_1(X)\Phi+I_2(X)\Phi e_{-2})+\text{c.c.}+\text{h.o.t.}\end{aligned}\tag{14}$$

where $\alpha=3+\mathrm{i}\beta$, $X_0=-\mathrm{i}\pi/b_2$, p_1,p_2 are (undetermined) real constants, and

$$I_1(X)=\left(R_0'\int_{X_0}^X\frac{1}{R_0'^2}\mathrm{d}T+\mathrm{i}R_0\int_{X_0}^X R_0R_0'\int_{X_0}^S\frac{1}{R_0'^2}\mathrm{d}T\mathrm{d}S\right)\mathrm{e}^{\mathrm{i}\Theta_0},$$

$$I_2(X)=\left(R_0'\int_{X_0}^X\frac{1}{R_0'^2}\mathrm{d}T+\mathrm{i}R_0\int_{X_0}^X R_0R_0'\int_{X_0}^S\frac{1}{R_0'^2}\mathrm{d}T\mathrm{d}S\right)\mathrm{e}^{-\mathrm{i}\Theta_0}.$$

This theorem shows that for $n \to \infty$ the series diverges due to $\Gamma\left(\frac{n}{2}+\alpha\right)$, but for X large the divergence is slow due to the factor $(X_j - X)^{-\frac{n+1}{2}+\alpha}$ and one can already see here that the error by truncation will decrease rapidly for $|X| \to \infty$.

Proof. Pursuing the calculation in (8) the equation for U_n at ε^n is

$$0 = \sum_{s=0}^{\lfloor \frac{n-1}{4} \rfloor} L_{4s} U_{n-4s} + L_2 U_{n-2} + \sum_{s=0}^{\lfloor \frac{n-1}{2} \rfloor} \sum_{m=2}^{\infty} \sum_{\substack{s_1+\ldots+s_m=n-2s \\ 0<s_i}} F^m_{2s}(U_{s_1}, ..., U_{s_m}). \quad (15)$$

W.l.o.g., this results, see remark 3.2, in $U_n = \sum_{k=-\infty}^{\infty} A_{n,k}(X)\Phi_{n,k}e_k(x)$ with almost all $A_{n,k} \equiv 0$ and (15) can be transformed into a recurrent set of equations for $A_{n,k}\Phi_{n,k}$. As these equations need to be solved in the limit $n \to \infty$ we need a simplification to get rid of the nested sum. The key idea is to make an ansatz for $A_{n,k}\Phi_{n,k}$ in such a way, that we can derive its leading order form by an expansion of inverse powers of n. The ansatz we use reads

$$A_{n,k}\Phi_{n,k} \underset{n\to\infty}{\sim} \sum_{j\in\mathbb{Z}} \frac{\kappa^n \Gamma(\frac{n}{2}+\alpha_k)}{(X_j - X)^{\frac{n+1}{2}+\alpha_k}} \left(h^0_k(X) + \frac{1}{n} h^1_k(X) + ... \right) =: \sum_{j\in\mathbb{Z}} \frac{H_{n,k}(X)}{(X_j - X)^{\frac{n+1}{2}+\alpha_k}}, \quad (16)$$

with $\alpha_k, \kappa \in \mathbb{C}$ to be determined, $X_j = \mathrm{i}(2j+1)\pi/b_2$, for a fixed $j \in \mathbb{Z}$, and $h^l_k : \mathbb{C} \to \mathbb{C}^2, l \in \mathbb{N}_0$ are functions independent of n. This is motivated by the fact that $A_{n,k}$ should have the same singularities X_j as $A_{1,1}$, which has the asymptotic behavior

$$A_{1,1} \underset{X\to X_j}{\sim} \frac{\tilde{H}_{1,1}}{(X_j - X)^{\frac{1}{2}+\mathrm{i}\beta}}$$

with a constant $\tilde{H}_{1,1}$. The power of $(X_j - X)$ in (16) is necessary, because the second derivative of $A_{n-2,k}$ and forth derivative of $A_{n-4,k}$ are used to determine $A_{n,k}$. The independence of $H_{n,k}(X)$ from X_j is not imposed, but a natural consequence of the $2\pi\mathrm{i}$ periodicity of the exponential function. The linear nature of all calculations allows us to compute the behavior separately for each singularity and add these contributions in the end. In detail we will only need to add the contributions of X_0 and X_{-1} in the limit $n \to \infty$ as these are the dominant ones on the real line for $n \to \infty$ by the factor $(X_j - X)^{\frac{n+1}{2}+\alpha_k}$. Thus our ansatz reads for now

$$A_{n,k}\Phi_{n,k} \underset{n\to\infty}{\sim} \frac{\kappa^n \Gamma(\frac{n}{2}+\alpha_k)}{(X_0 - X)^{\frac{n+1}{2}+\alpha_k}} \left(h^0_k(X) + \frac{1}{n} h^1_k(X) + ... \right) =: \frac{H_{n,k}(X)}{(X_0 - X)^{\frac{n+1}{2}+\alpha_k}}. \quad (17)$$

The calculations will show, that the contribution of $A_{n,k}\Phi_{n,k}|_{X_{-1}}$ is equal to $\bar{A}_{n,-k}\Phi_{n,-k}\big|_{X_0}$, and as explained above we can add that later.

Inserting (17) in the recurrent set of equation (15) and multiplying the result by $(X_0 - X)^{\frac{n+1}{2}+\alpha_k}$ we get

$$
\begin{aligned}
0 = {} & L_0 H_{n,k} + \mathrm{i}2kk_c \frac{n-2+\alpha_k}{2} D H_{n-2,k} \\
& + \frac{n-4+\alpha_k}{2}\frac{n-2+\alpha_k}{2} D H_{n-4,k} \\
& + \sum_{m=2}^{\infty} \sum_{\substack{s_1+\ldots+s_m=n \\ 0<s_i}} \sum_{k_1+\ldots+k_m=k} F_0^m(H_{s_1,k_1},\ldots,H_{s_m,k_m})(X_0-X)^{-\frac{m-1}{2}-\sum_{j=1}^m \alpha_{k_0}+\alpha_k} \\
& + O\left(\Gamma\left(\frac{n}{2}-1+\alpha_k\right)\right). \qquad (18)
\end{aligned}
$$

We divide this by $\Gamma(\frac{n}{2}+\alpha_k)$ and can start an asymptotic expansion of $H_{n,k}$ in inverse powers of n. The nested sum also contains different magnitudes of n, and so there are no infinite sums in the leading orders equations. The factors $(X_0-X)^{-\frac{m-1}{2}-\sum_{j=1}^m \alpha_{k_j}+\alpha_k}$ will vanish for the interesting values of k, which are the dominant modes and which we investigate now. These are the modes with maximal real part of $\alpha_k =: \alpha$. We will see that the imaginary part of α is not constant, and thus the notation $\alpha_k = \alpha$ for all dominant α_k seems to be misleading, but indeed there is an α such that all dominant contributions can be expressed with α and $\bar{\alpha}$, which then justifies the loose notation. The restriction to dominant modes does not imply any extra assumptions, as we do not restrict the total number of dominant modes.

At the dominant modes the leading order equation in (18) is

$$0 = \left(\kappa^4 L_0(k,\lambda_c) + \mathrm{i}2kk_c\kappa^2 D + D\right) h_k^0.$$

We seek solutions $h_k^0 \not\equiv 0$ as $h_k^0 \equiv 0$ would be equivalent to a reduction of α. Thus we need $\mathcal{L} := \left(\kappa^4 L_0(k,\lambda_c) + \mathrm{i}2kk_c\kappa^2 D + D\right)$ to be singular. As $L_0(k,\lambda_c) = J(\lambda_c) - k^2 k_c^2 D$ this is the case if and only if

$$-k^2k_c^2\kappa^4 + \mathrm{i}2kk_c\kappa^2 + 1 = -k_c^2\kappa^4, \qquad (19)$$

and $\mathcal{L}$ then has the nontrivial kernel vector $h_k^0(X) = \tilde{h}_k^0(X)\Phi$ with a scalar function $\tilde{h}_k^0$, which we denote by h_k^0 again. The solutions to (19) are $\kappa^2 = \mathrm{i}/k_c(k\pm 1)$ for $k \neq \pm 1$, for $k=-1$ we have the double root $\kappa^2 = \mathrm{i}/k_c(k-1)$ and for $k=1$ we have the double root $\kappa^2 = \mathrm{i}/k_c(k+1)$. This shows that $k = 0, \pm 2$ are the dominant modes, as κ has the biggest absolute values for these. Hence we use the ansatz $\alpha_0 = \alpha_{\pm 2} = \alpha$, $\alpha_{\pm 1} = \alpha_{\pm 3} = \alpha - \frac{1}{2}$, $\alpha_{\pm 4} = \alpha - 1$, $\ldots$ with still unknown α, to get the right balance between the modes, i.e. to eliminate the $(X_0-X)^{-\frac{m-1}{2}-\sum_{j=1}^m \alpha_{k_j}+\alpha_k}$ factor in (18). Formally we would need to differ between $\kappa^2 = \mathrm{i}/k_c$ and $\kappa^2 = -\mathrm{i}/k_c$, as either $k=2$ or $k=-2$ is the only dominant mode along with $k=0$, but our ansatz above will give the same results with clearer calculations and just yields, depending on k, either $h_2^0 = 0$ or $h_{-2}^0 = 0$.

The calculation of α_k and h_k^0 for the dominant modes is cumbersome and does not yield additional insights, and thus we only describe the method briefly and state the results. The basic calculus is to investigate (18) in higher powers of $\frac{1}{n}$. At $O\left(\frac{1}{n}\right)$ there is exact cancellation for arbitrary α_k and h_k^0, thus no information is gathered. At $O\left(\frac{1}{n^2}\right)$ there are two cases. For $\kappa^2 = \mathrm{i}/k_c$ the modes 2 and 0 are dominant and h_0^0, h_2^0 have to satisfy

$$0 = \eta_0\partial_X^2 h_2^0 + \eta_1 h_2^0 + \eta_2|A|^2 h_2^0 + \eta_3 A_{1,1}^2 h_0^0 + \eta_4|A|^4 h_2^0 + \eta_5|A|^2 A_{1,1}^2 h_0^0 + \mathrm{i}\eta_6 A^2\partial_X h_0^0 + \mathrm{i}\eta_7 A h_2^0\partial_X\bar{A}$$
$$+ \mathrm{i}\eta_8|A|^2\partial_X h_k 2^0 + \mathrm{i}\eta_9 h_0^0 A\partial_X A + \mathrm{i}\eta_{10} h_2^0\bar{A}\partial_X A,$$

and its complex conjugated equation, which are the linearized amplitude equations which will be derived in section 4.2, see (23), where we also explain the constants η_j. For $\kappa^2 = -i/k_c$ the same equations have to hold for h^0_{-2} and h^0_0. We derive the solutions to this equation in section 4.2 as well, and obtain

$$\bar{h}_0^0 = h_2^0 = K_2 A' + \mathrm{i}K_4 A + \left(R_0'\int_{X_0}^X \frac{K_1R_0^2 + K_3}{R_0'^2}\mathrm{d}T + \mathrm{i}2\hat{c}K_1R_0\int_{X_0}^X\frac{1}{R_0^2}\mathrm{d}T\right.$$
$$\left.+\mathrm{i}2\hat{c}R_0\int_{X_0}^X R_0R_0'\int_{X_0}^S\frac{K_1R_0^2+K_3}{R_0'^2}\mathrm{d}T\mathrm{d}S\right)\mathrm{e}^{\mathrm{i}\Theta_0}$$

with A, R_0, Θ_0 from theorem 3.1, $\hat{c} = -\frac{c_4+c_5}{4c_0}$, c_0, c_4, c_5 from the proof of theorem 3.1 and yet unknown constants K_i in the case $\kappa^2 = \mathrm{i}/k_c$. The solutions to h^0_{-2}, h^0_0 for $\kappa^2 = -\mathrm{i}/k_c$ are given by the map $\left(h_0^0, h_2^0\right) \to \left(h^0_{-2}, h_0^0\right)$. To examine the dominant contributions we investigate these solutions in the limit $X \to X_0$ and find

$$A' \underset{X\to X_0}{\sim} \text{const.}(X_0 - X)^{-\frac{3}{2}+\mathrm{i}\beta},$$
$$A \underset{X\to X_0}{\sim} \text{const.}(X_0 - X)^{-\frac{1}{2}+\mathrm{i}\beta},$$
$$\left(R_0'\int_{X_0}^X\frac{R_0^2}{R_0'^2}\mathrm{d}T + \mathrm{i}\left(R_0\int_{X_0}^X R_0R_0'\int_{X_0}^S\frac{R_0^2}{R_0'^2}\mathrm{d}T\mathrm{d}S + R_0\int_{X_0}^X\frac{1}{R_0^2}\mathrm{d}T\right)\right)\mathrm{e}^{\mathrm{i}\Theta_0} \underset{X\to X_0}{\sim} \text{const.}(X_0 - X)^{\frac{3}{2}+\mathrm{i}\beta},$$
$$\left(R_0'\int_{X_0}^X\frac{1}{R_0'^2}\mathrm{d}T + \mathrm{i}R_0\int_{X_0}^X R_0R_0'\int_{X_0}^S\frac{1}{R_0'^2}\mathrm{d}T\mathrm{d}S\right)\mathrm{e}^{\mathrm{i}\Theta_0} \underset{X\to X_0}{\sim} \text{const.}(X_0 - X)^{\frac{5}{2}+\mathrm{i}\beta}.$$

Thus the solution with maximal possible α is the solution with constant K_3, as for $X \to X_0$ the ansatz (17) implies for example $A_{n,2} \underset{X\to X_0}{\sim} \text{const.}(X_0 - X)^{-\frac{n+1}{2}-\alpha+\frac{5}{2}+\mathrm{i}\beta}$ for $\kappa^2 = \mathrm{i}/k_c$ and we already argued that $A_{n,k} \underset{X\to X_0}{\sim} \text{const.}(X_0 - X)^{-\frac{n}{2}+\mathrm{i}k\beta}$. This yields $\alpha = 3 + \mathrm{i}\beta$. For $\kappa^2 = -\mathrm{i}/k_c$ we obtain $\alpha = 3 - \mathrm{i}\beta$ with the same argument. For convenience we set $\alpha = 3 + \mathrm{i}\beta$ and write $\bar{\alpha}$ for the other value. In summary we have

$$\bar{h}_0^0 = h_2^0 = K_3\left(R_0'\int_{X_0}^X\frac{1}{R_0'^2}\mathrm{d}T + \mathrm{i}R_0\int_{X_0}^X R_0R_0'\int_{X_0}^S\frac{1}{R_0'^2}\mathrm{d}T\mathrm{d}S\right)\mathrm{e}^{\mathrm{i}\Theta_0} + \text{h.o.t.}$$

for $\kappa^2 = \mathrm{i}/k_c$, and

$$\bar{h}^0_{-2} = h_0^0 = K_3\left(R_0'\int_{X_0}^X\frac{1}{R_0'^2}\mathrm{d}T + \mathrm{i}R_0\int_{X_0}^X R_0R_0'\int_{X_0}^S\frac{1}{R_0'^2}\mathrm{d}T\mathrm{d}S\right)\mathrm{e}^{\mathrm{i}\Theta_0} + \text{h.o.t.}$$

for $\kappa^2 = -\mathrm{i}/k_c$. Note that $\kappa^2 = \pm\mathrm{i}/k_c$ implies four solutions $\kappa = \pm\sqrt{\pm\mathrm{i}/k_c}$ which have to be investigated, but, besides the arbitrary constants, the solutions to the same κ^2 result in a $(-1)^n$ difference only. Furthermore we can choose $A_{2,1} = 0$, as there is no inhomogeneous term if we

continue (8) to ε^6, and thus every $A_{n,k}$ with $n+k$ odd is zero and the arbitrary constants of both solutions for $\kappa^2 = \mathrm{i}/k_c$ and for $\kappa^2 = -\mathrm{i}/k_c$ respectively, must match to ensure this symmetry. We call the remaining arbitrary constant p_1 for $\kappa^2 = \mathrm{i}/k_c$ and p_2 for $\kappa^2 = -\mathrm{i}/k_c$. All in all this yields the large n behavior

$$U_n \underset{n\to\infty}{\sim} p_1 \left(\frac{\mathrm{e}^{\mathrm{i}\frac{\pi}{4}}}{\sqrt{k_c}}\right)^n \frac{\Gamma(\frac{n}{2}+\alpha)}{(X_0-X)^{\frac{n+1}{2}+\alpha}}(1+(-1)^n)\,(I_2(X)\Phi + I_1(X)\Phi e_2) + p_2 \left(\frac{\mathrm{e}^{\mathrm{i}\frac{3\pi}{4}}}{\sqrt{k_c}}\right)^n \frac{\Gamma(\frac{n}{2}+\bar{\alpha})}{(X_0-X)^{\frac{n+1}{2}+\bar{\alpha}}}(1+(-1)^n)\,(I_1(X)\Phi + I_2(X)\Phi e_{-2}) + \text{c.c.}$$

with $I_1 = \left(R_0' \int_{X_0}^X \frac{1}{R_0'^2}\mathrm{d}T + \mathrm{i}R_0 \int_{X_0}^X R_0 R_0' \int_{X_0}^S \frac{1}{R_0'^2}\mathrm{d}T\mathrm{d}S\right)\mathrm{e}^{\mathrm{i}\Theta_0}$ and $I_2 = \left(R_0' \int_{X_0}^X \frac{1}{R_0'^2}\mathrm{d}T + \mathrm{i}R_0 \int_{X_0}^X R_0 R_0' \int_{X_0}^S \frac{1}{R_0'^2}\mathrm{d}T\mathrm{d}S\right)\mathrm{e}^{-\mathrm{i}\Theta_0}$. The complex conjugated must be added by the influence of the singularity X_{-1} by symmetry. □

As mentioned above theorem 4.1 shows that the series has to be truncated and we now discuss its remainder. Before talking about the remainder by truncation, we take a look at the remainder by deviation from the Maxwell point λ_M. Here we also derive the linearized version of the amplitude equation and its solutions, already used to derive $I_{1,2}$.

4.2. Contribution to the remainder by the deviation from the Maxwell point

We deal with the estimation of the error of the asymptotic expansion (5) now. As noted earlier, this has two contributions: the error R_N^T by truncation, and the error R^{λ_δ} by $\varepsilon^4\lambda_\delta$, the deviation from the Maxwell point. The full error is given by $R_N^T + \varepsilon R_N^{\lambda_\delta}$ in leading order, where the rescaling is for convenience only. The aim of this section is to estimate the error R_N^T, i.e. to prove the following theorem.

Theorem 4.2. *Let (5) be an asymptotic expansion of a front solution U_ε^f as in hypothesis 2.2. If $\left|R_N^T\right| \ll \left|R^{\lambda_\delta}\right|$, then R^{λ_δ}, i.e. the error by a change in λ_δ, satisfies*

$$R^{\lambda_\delta}(x,X) \underset{\varepsilon\to 0}{\sim} R_{1,1}^{\lambda_\delta}(X)\Phi e_1(x) + \text{c.c.} + \text{h.o.t.}$$

where

$$R_{1,1}^{\lambda_\delta}(X) = K_2 A' + \mathrm{i}K_4 A + \left(R_0' \int_{X_0}^X \frac{K_1 R_0^2 + K_3}{R_0'^2}\mathrm{d}T + \mathrm{i}2\hat{c}K_1 R_0 \int_{X_0}^X \frac{1}{R_0^2}\mathrm{d}T + \mathrm{i}2\hat{c}R_0 \int_{X_0}^X R_0 R_0' \int_{X_0}^S \frac{K_1 R_0^2 + K_3}{R_0'^2}\mathrm{d}T\mathrm{d}S\right)\mathrm{e}^{\mathrm{i}\Theta_0} + \left(\frac{2\sqrt{15}}{c_0}\lambda_\delta R_0' \int_0^X \frac{R_0^2}{R_0'^2}\mathrm{d}T + \mathrm{i}2\hat{c}\frac{2\sqrt{15}}{c_0}\lambda_\delta R_0 \int_0^X R_0 R_0' \int_{X_0}^S \frac{R_0^2}{R_0'^2}\mathrm{d}T\mathrm{d}S\right)\mathrm{e}^{\mathrm{i}\Theta_0} \tag{20}$$

with real constants $\hat{c}, c_0$ and (yet arbitrary) constants $K_1, \ldots K_4$.

Note that R_0 does not denote any error term, but the modulus of the leading order amplitude A, which is calculated in section 3.

Proof. Under the assumption of theorem 4.2 and with the λ-scaling (6) equation (7), which was derived in the leading order calculation, reduces to

$$-\varepsilon^5(\partial_\lambda J)(\lambda_c)\lambda_\delta(U_1+...) = \varepsilon L(\partial_x,\varepsilon^2\partial_X,\lambda_c)R^{\lambda_\delta} + \sum_{k=2}^{\infty}\varepsilon^k F_0^k[\lambda_c,\sigma_0](U_0^{k-1},R^{\lambda_\delta}) + \varepsilon^2\sum_{k=2}^{\infty}\varepsilon^k F_2^k[\lambda_c,\sigma_0](U_0^{k-1},R^{\lambda_\delta})+\dots \tag{21}$$

where $L(\partial_x,\varepsilon^2\partial_X,\lambda_c)$ denotes all linear parts. Higher order terms in ε along with $O({R^{\lambda_\delta}}^2)$ terms are denoted as '…'. We want to examine the remainder in regions where it is exponential small, and thus get a good approximation for $R_N^{\lambda_\delta}$ with the leading order solution of another multi-scale ansatz. Thus we write

$$R_N^{\lambda_\delta}(x,X) = R_1^{\lambda_\delta}(x,X) + \varepsilon R_2^{\lambda_\delta}(x,X)+\dots. \tag{22}$$

With ansatz (22) the equations at $\varepsilon^l, l<5$ in (21) are the linearized versions of the equations derived in section 3 and yield $R_1^{\lambda_\delta} = R_{1,1}^{\lambda_\delta}e_1 + R_{1,-1}^{\lambda_\delta}e_{-1}$ with arbitrary $R_{1,\pm1}^{\lambda_\delta}$. At ε^5 the leading order of the inhomogeneous addend $-\varepsilon^5(\partial_\lambda J)(\lambda_c)\lambda_\delta(U_1+...)$ arises and at $\varepsilon^5 e_1$ we have

$$\begin{aligned}-A_{1,1}\langle(\partial_\lambda J)(\lambda_c)\lambda_\delta\Phi,\Phi_\perp\rangle = {}& \eta_0\partial_X^2R_{1,1}^{\lambda_\delta}+\eta_1R_{1,1}^{\lambda_\delta}+\eta_2|A|^2R_{1,1}^{\lambda_\delta}+\eta_3A_{1,1}^2R_{1,-1}^{\lambda_\delta}+\eta_4|A|^4R_{1,1}^{\lambda_\delta}\\ &+\eta_5|A|^2A_{1,1}^2{R^{\lambda_\delta}}_{1,-1}+\mathrm{i}\eta_6A^2\partial_X{R^{\lambda_\delta}}_{1,-1}+\mathrm{i}\eta_7A{R^{\lambda_\delta}}_{1,1}\partial_X\bar{A}\\ &+\mathrm{i}\eta_8|A|^2\partial_X{R^{\lambda_\delta}}_{1,1}+\mathrm{i}\eta_9{R^{\lambda_\delta}}_{1,-1}A\partial_XA+\mathrm{i}\eta_{10}{R^{\lambda_\delta}}_{1,1}\bar{A}\partial_XA,\end{aligned} \tag{23}$$

where η_j are real constants which can be expressed through the c_j of section 3, see (11), by

$$c_0=\eta_0,\ c_1=\eta_1,\ 3c_2=\eta_2,\ 2c_2=\eta_3,\ 3c_3=\eta_4,\ 2c_3=\eta_5,$$
$$c_4=\eta_6,\ 2c_4=\eta_7,\ c_5=\eta_8,\ c_5=\eta_9,\ c_5=\eta_{10}.$$

At e_{-1} the complex conjugated equation arises with $R_{1,1}^{\lambda_\delta}$ and $R_{1,-1}^{\lambda_\delta}$ being exchanged and thus $R_{1,-1}^{\lambda_\delta}=\bar{R}_{1,1}^{\lambda_\delta}$. For the homogeneous equation one can immediately spot the two solutions A and A'. Further solutions can be derived by reduction of order for which the complex equation needs to be transformed into real ones via the ansatz $R_{1,1}^{\lambda_\delta}=(R_1+\mathrm{i}R_0\Theta_1)\,\mathrm{e}^{\mathrm{i}\Theta_0}$ with unknown real functions R_1,Θ_1. The solution $R_{1,1}^{\lambda_\delta}=A'$ corresponds to $R_1=R_0'$, $\Theta_1=\Theta_0'$ and $R_{1,1}^{\lambda_\delta}=\mathrm{i}A$ corresponds to $\Theta_1=1$, $R_1=0$. The full solution of the homogeneous equation thus is given by

$$\begin{aligned}(R_1+\mathrm{i}R_0\Theta_1)\,\mathrm{e}^{\mathrm{i}\Theta_0} = {}& K_2A'+\mathrm{i}K_4A+\Bigg(R_0'\int_{X_0}^{X}\frac{K_1R_0^2+K_3}{R_0'^2}\mathrm{d}T\\ &+\mathrm{i}2\hat{c}K_1R_0\int_{X_0}^{X}\frac{1}{R_0^2}\mathrm{d}T+\mathrm{i}2\hat{c}R_0\int_{X_0}^{X}R_0R_0'\int_{X_0}^{S}\frac{K_1R_0^2+K_3}{R_0'^2}\mathrm{d}T\mathrm{d}S\Bigg)\mathrm{e}^{\mathrm{i}\Theta_0}\end{aligned}$$

with real constants K_j and $\hat{c}=-\frac{c_4+c_5}{4c_0}$. One specific solution of the inhomogeneous equation can then be found as

$$\left(\frac{2\sqrt{15}}{c_0}\lambda_\delta R_0'\int_0^X\frac{R_0^2}{R_0'^2}\mathrm{d}T+\mathrm{i}2\hat{c}\frac{2\sqrt{15}}{c_0}\lambda_\delta R_0\int_0^X R_0R_0'\int_{X_0}^{S}\frac{R_0^2}{R_0'^2}\mathrm{d}T\mathrm{d}S\right)\mathrm{e}^{\mathrm{i}\Theta_0}.$$

□

The term which is proportional to λ_δ is exponential growing for $X \to \infty$. Thus $K_1, \ldots, K_4 = 0$ is no appropriate choice. For $X \to \infty$ the choice $K_3 = O(\lambda_\delta)$ would bound the remainder, as $R_0 = O(1)$ for $X \to \infty$. But the factor of K_3 is unbounded for $X \to -\infty$. Thus there is no global choice of constants to bound the remainder uniformly, and indeed we will see that the error is non dominant in an $X = O(\varepsilon)$ regime, where the error by truncation dominates, which allows a switching from $K_3 = 0$ for $X \to -\infty$ to $K_3 = O(\lambda_\delta)$ for $X \to \infty$. This way a uniformly exponentially small remainder (in leading order) can be established via a matching of the two errors for λ_δ sufficiently small.

4.3. Truncation error terms in the remainder

We derive the truncation error now, which is determined up to some arbitrary real constants just like the deviation error. The arbitrary constants of both errors are then determined by a matching process in section 4.4. To establish the truncation error R_N^T an appropriate truncation order N has to be determined.

Lemma 4.3. *Let (5) be an asymptotic expansion of a front solution U_ε^f as in hypothesis 2.2. Then the optimal truncation point N, for which consecutive terms are of the same magnitude, is given by*

$$N = N(X, \varepsilon) \underset{\varepsilon \to 0}{\sim} \frac{2k_c\,|X - X_0|}{\varepsilon^2} - 2\alpha.$$

Proof. At first glance we have to find n such that $\frac{\varepsilon^{n+1} U_{n+1}}{\varepsilon^n U_n} = 1$, but if we assume that the truncation point $N \to \infty$ for $\varepsilon \to 0$, which is a natural assumption, theorem 4.1 can be applied, and shows that $U_n \equiv 0$ in leading order for n odd. Thus we consider the equation

$$\frac{\varepsilon^{n+2} U_{n+2}}{\varepsilon^n U_n} = 1. \tag{24}$$

instead. We also w.l.o.g. choose $N + 1 \in 2\mathbb{Z}$ for this reason. Evaluating (24) by the use of (14) we have

$$N + 1 \underset{N \to \infty}{\sim} \frac{2k_c |X_0 - X|}{\varepsilon^2} - 2\alpha, \tag{25}$$

what had to be proven and is in accordance with our assumption, as indeed $N \to \infty$ for $\varepsilon \to 0$. □

With the optimal truncation point we can formulate theorem 4.4, which describes R_N^T, the error by truncation.

Theorem 4.4. *Let (5) be an asymptotic expansion of a front solution U_ε^f as in hypothesis 2.2, with N from lemma 4.3, and let $X_0 - X = r\mathrm{e}^{\mathrm{i}\left(\frac{\pi}{2} + \varepsilon\hat{\theta}\right)}$, $r \in \mathbb{R}_+, \hat{\theta} \in \mathbb{R}$. Then the truncation error R_N^T at $\lambda_\delta = 0$ is given by*

$$R_N^T(x, X) = R_N^T(x, r, \hat{\theta}) \underset{\varepsilon \to 0}{\sim} S_0(r, \hat{\theta}) e_1(x) + \text{c.c.} + \text{h.o.t.}$$

with

$$S_0(r, \hat{\theta}) \underset{\varepsilon \to 0}{\sim} -\pi\sqrt{2}|p_1| r^{-\frac{1}{2}} k_c^3 \mathrm{e}^{\mathrm{i}k_c \frac{X_0}{\varepsilon^2}} \mathrm{e}^{-\frac{1}{2}\pi\beta} \mathrm{e}^{-k_c r\hat{\theta}^2} I_1(X_0 - \mathrm{i}r)\, \mathrm{erf}(\sqrt{k_c r}\hat{\theta}) \sin(\ln(k_c)\beta + \arg(p_1) + \omega)(C_1 + \bar{C}_{-1}),$$

where $\operatorname{erf}(x) = (2/\sqrt{\pi})\int_0^x \mathrm{e}^{-t^2}\mathrm{d}t$ *is the error function,* ω *is the phase shift, already introduced in theorem 3.1, and* C_1, C_{-1} *are (yet arbitrary) constants.*

Proof. The ansatz $U = \sum_{k=1}^{N} \varepsilon^k U_k + R_N^T$ yields the equation

$$0 = \varepsilon^{N+1} 2D\partial_x\partial_X U_{N-1} + \varepsilon^{N+1} D\partial_X^2 U_{N-3} + \varepsilon^{N+3} D\partial_X^2 U_{N-1} + \varepsilon^{N+1}\text{nonlinearities in } U + (J(\lambda_c) + \partial_x^2 D)R_N^T + \varepsilon^2 2D\partial_x\partial_X R_N^T + \varepsilon^4 D\partial_X^2 R_N^T + \sum_{k=2}^{\infty} F^k[\lambda,\sigma](U^{k-1}, R_N^T) + O({R_N^T}^2). \tag{26}$$

Neglecting the $O({R_N^T}^2)$ terms, this again can be solved with a multi scales ansatz for R_N^T for which we need to find the leading order in ε first. As $N = O\left(\frac{1}{\varepsilon^2}\right)$ we have $\partial_X = O(\frac{1}{\varepsilon^2})$ and $U_{n-1} = O(\varepsilon^2 U_{n+1})$. Thus the leading order terms are given by

$$\varepsilon^{N+1} 2\partial_x\partial_X D U_{N-1} + \varepsilon^{N+1}\partial_X^2 D U_{N-3} + \varepsilon^{N+3}\partial_X^2 D U_{N-1}. \tag{27}$$

The next step is to use the asymptotic for N. As all calculations will be linear we can assume that we have

$$U_N \underset{N\to\infty}{\sim} p_1 \left(\frac{\mathrm{e}^{\mathrm{i}\frac{\pi}{4}}}{\sqrt{k_c}}\right)^N \frac{\Gamma(\frac{N}{2}+\alpha)}{(X_0 - X)^{\frac{N}{2}+\alpha}}(1 + (-1)^N)\,(I_2\Phi + I_1\Phi e_2)$$

by theorem 4.1 and add the contributions of p_2 and the complex conjugated later. More precisely we will see that there is no contribution of p_2 at leading order and we have to add the complex conjugated only. Then, to prepare for a multi scales ansatz, we write $\varepsilon^{N+1} U_{N-1} \underset{N\to\infty}{\sim} \eta\,(I_2\Phi + I_1\Phi e_2)$, where η depends on N, X and ε, and factor out η in all contributions. We have

$$\varepsilon^{N+1} 2\partial_x\partial_X D U_{N-1} \underset{N\to\infty}{\sim} \mathrm{i}4k_c \frac{\frac{N-1}{2}+\alpha}{X_0 - X}\eta I_1 e_2 D\Phi,$$

$$\varepsilon^{N+1}\partial_X^2 D U_{N-3} \underset{N\to\infty}{\sim} \left(\frac{\mathrm{e}^{\mathrm{i}\frac{\pi}{4}}}{\sqrt{k_c}}\right)^{-2} \frac{\frac{N-1}{2}+\alpha}{X_0 - X}\eta\,(I_2 + I_1 e_2)\,D\Phi,$$

$$\varepsilon^{N+3}\partial_X^2 D U_{N-1} \underset{N\to\infty}{\sim} \varepsilon^2 \frac{\left(\frac{N-1}{2}+\alpha\right)\left(\frac{N+1}{2}+\alpha\right)}{(X_0 - X)^2}\eta\,(I_2 + I_1 e_2)\,D\Phi.$$

We write

$$X_0 - X = r\mathrm{e}^{\mathrm{i}\theta + \mathrm{i}\pi} = r\mathrm{e}^{\mathrm{i}(-\frac{\pi}{2} + \varepsilon\hat{\theta}) + \mathrm{i}\pi}, \tag{28}$$

with $r \in \mathbb{R}_+$ and $\hat{\theta} \in \mathbb{R}$, where it will be motivated to write $\theta = -\frac{\pi}{2} + \varepsilon\hat{\theta}$ by the investigation of the factor η later. With this and by applying the asymptotic for $N \to \infty$ we obtain

$$\varepsilon^{N+1} 2\partial_x\partial_X D U_{N-1} \underset{N\to\infty}{\sim} \mathrm{i}4k_c^2\varepsilon^{-2}(-\mathrm{i})\mathrm{e}^{-\mathrm{i}\varepsilon\hat{\theta}}\eta I_1 e_2 D\Phi + O(\eta),$$

$$\varepsilon^{N+1}\partial_X^2 D U_{N-3} \underset{N\to\infty}{\sim} k_c^2\varepsilon^{-2}(-\mathrm{i})(-\mathrm{i})\mathrm{e}^{-\mathrm{i}\varepsilon\hat{\theta}}\eta\,(I_2 + I_1 e_2)\,D\Phi + O(\eta),$$

$$\varepsilon^{N+3}\partial_X^2 D U_{N-1} \underset{N\to\infty}{\sim} k_c^2\varepsilon^{-2}(-\mathrm{i})^2\mathrm{e}^{-\mathrm{i}2\varepsilon\hat{\theta}}\eta\,(I_2 + I_1 e_2)\,D\Phi + O(\eta).$$

As $\varepsilon \to 0$ implies $N \to \infty$ by (25) we can apply the above results in the limit $\varepsilon \to 0$ and use $\mathrm{e}^{i\varepsilon\hat{\theta}} = 1 + \mathrm{i}\varepsilon\hat{\theta} + O(\varepsilon^2)$ to obtain

$$\begin{aligned}
&\varepsilon^{N+1} 2\partial_x \partial_X D U_{N-1} \underset{\varepsilon\to 0}{\sim} 4k_c^2 \varepsilon^{-2} \left(1 - \mathrm{i}\varepsilon\hat{\theta} + O(\varepsilon^2)\right) \eta I_1 e_2 D\Phi + O(\eta),\\
&\varepsilon^{N+1} \partial_X^2 D U_{N-3} \underset{\varepsilon\to 0}{\sim} -k_c^2 \varepsilon^{-2} \left(1 - \mathrm{i}\varepsilon\hat{\theta} + O(\varepsilon^2)\right) \eta \left(I_2 + I_1 e_2\right) D\Phi + O(\eta),\\
&\varepsilon^{N+3} \partial_X^2 D U_{N-1} \underset{\varepsilon\to 0}{\sim} -k_c^2 \varepsilon^{-2} \left(1 - \mathrm{i}2\varepsilon\hat{\theta} + O(\varepsilon^2)\right) \eta \left(I_2 + I_1 e_2\right) D\Phi + O(\eta).
\end{aligned} \tag{29}$$

It remains to determine η in the limit $\varepsilon \to 0$. We have

$$\eta = \varepsilon^{N+1} p_1 2 \left(\frac{\mathrm{e}^{\mathrm{i}\frac{\pi}{4}}}{\sqrt{k_c}}\right)^{N-1} \frac{\Gamma(\frac{N-1}{2} + \alpha)}{(X_0 - X)^{\frac{N-1}{2}+\alpha}} = \varepsilon^{N+1} p_1 \frac{-2\mathrm{i}k_c \left(X_0 - X\right)}{\frac{N-1}{2} + \alpha} \left(\frac{\mathrm{e}^{\mathrm{i}\frac{\pi}{4}}}{\sqrt{k_c}}\right)^{N+1} \frac{\Gamma(\frac{N+1}{2} + \alpha)}{(X_0 - X)^{\frac{N+1}{2}+\alpha}}.$$

Applying Stirling's approximation for $N \to \infty$ respectively $\varepsilon \to 0$, we obtain

$$\eta \underset{\varepsilon\to 0}{\sim} \varepsilon^{N+1} p_1 \frac{-2\mathrm{i}k_c \left(X_0 - X\right)}{\frac{N-1}{2} + \alpha} \left(\frac{\mathrm{e}^{\mathrm{i}\frac{\pi}{4}}}{\sqrt{k_c}}\right)^{N+1} \frac{\sqrt{\frac{2\pi}{\frac{N+1}{2}+\alpha}} \left(\frac{\frac{N+1}{2}+\alpha}{e}\right)^{\frac{N+1}{2}+\alpha}}{(X_0 - X)^{\frac{N+1}{2}+\alpha}}.$$

With (25) and (28) this results in

$$\begin{aligned}
&\eta \underset{\varepsilon\to 0}{\sim} \varepsilon^{N+1} p_1 2\mathrm{i}\varepsilon^2 \mathrm{e}^{\mathrm{i}\theta} \left(\frac{\mathrm{e}^{\mathrm{i}\frac{\pi}{4}}}{\sqrt{k_c}}\right)^{\frac{2k_c r}{\varepsilon^2} - 2\alpha} \sqrt{2\pi\varepsilon^2 \frac{1}{k_c r}} \frac{\left(\frac{k_c r}{\varepsilon^2}\right)^{\frac{k_c r}{\varepsilon^2}} \mathrm{e}^{-\frac{k_c r}{\varepsilon^2}}}{(-r)^{\frac{k_c r}{\varepsilon^2}} \left(\mathrm{e}^{\mathrm{i}\theta}\right)^{\frac{k_c r}{\varepsilon^2}}}\\
&= \varepsilon^{N+1} p_1 2\mathrm{i}\varepsilon^2 \mathrm{e}^{\mathrm{i}\theta} \mathrm{i}^{\frac{k_c r}{\varepsilon^2} - \alpha} k_c^{-\left(\frac{k_c r}{\varepsilon^2} - \alpha\right)} \sqrt{2\pi}\varepsilon (k_c r)^{-\frac{1}{2}} \left(k_c r \varepsilon^{-2}\right)^{\frac{k_c r}{\varepsilon^2}} \mathrm{e}^{-\frac{k_c r}{\varepsilon^2}} (-r)^{-\frac{k_c r}{\varepsilon^2}} \left(\mathrm{e}^{\mathrm{i}\theta}\right)^{-\frac{k_c r}{\varepsilon^2}}\\
&= p_1 2\mathrm{i}\varepsilon^{3-2\alpha} \sqrt{2\pi} \mathrm{i}^{-\alpha} k_c^{\alpha} (k_c r)^{-\frac{1}{2}} (-\mathrm{i})^{\frac{k_c r}{\varepsilon^2}} \mathrm{e}^{-\frac{k_c r}{\varepsilon^2}} \mathrm{e}^{-\mathrm{i}\theta\left(\frac{k_c r}{\varepsilon^2} - 1\right)}.
\end{aligned}$$

Using (28) again, this finally yields

$$\eta \underset{\varepsilon\to 0}{\sim} p_1 2\varepsilon^{3-2\alpha} \sqrt{2\pi} \mathrm{i}^{-\alpha} k_c^{\alpha} (k_c r)^{-\frac{1}{2}} \mathrm{e}^{-\frac{k_c r}{\varepsilon^2}} \mathrm{e}^{-\mathrm{i}\varepsilon\hat{\theta}\left(\frac{k_c r}{\varepsilon^2} - 1\right)}. \tag{30}$$

The same calculation is valid for $\mathrm{e}^{\mathrm{i}\theta} = \mathrm{e}^{\mathrm{i}\left(\frac{\pi}{2} + \varepsilon\hat{\theta}\right)} = \mathrm{i}\mathrm{e}^{\mathrm{i}\varepsilon\hat{\theta}}$, but as we are interested in the behavior on the real line and X_0 is in the upper half plane, only the contribution of $\theta = -\frac{\pi}{2} + \varepsilon\hat{\theta}$ matters. At first glance the previous calculation suggests that the remainder is globally exponential small by the factor $\mathrm{e}^{-\frac{k_c r}{\varepsilon^2}}$. But indeed

$$\begin{aligned}
\mathrm{e}^{\mathrm{i}k_c x} &= \mathrm{e}^{\mathrm{i}k_c \frac{X}{\varepsilon^2}} \mathrm{e}^{\mathrm{i}\omega} = \mathrm{e}^{\mathrm{i}k_c \frac{X - X_0}{\varepsilon^2}} \mathrm{e}^{\mathrm{i}k_c \frac{X_0}{\varepsilon^2}} \mathrm{e}^{\mathrm{i}\omega} = \mathrm{e}^{\mathrm{i}k_c \frac{r\mathrm{e}^{\mathrm{i}\theta}}{\varepsilon^2}} \mathrm{e}^{\mathrm{i}k_c \frac{X_0}{\varepsilon^2}} \mathrm{e}^{\mathrm{i}\omega}\\
&= \mathrm{e}^{k_c \frac{r\mathrm{e}^{\mathrm{i}\varepsilon\hat{\theta}}}{\varepsilon^2}} \mathrm{e}^{\mathrm{i}k_c \frac{X_0}{\varepsilon^2}} \mathrm{e}^{\mathrm{i}\omega} = \mathrm{e}^{k_c \frac{r\mathrm{e}^{\mathrm{i}\varepsilon\hat{\theta}}}{\varepsilon^2}} \mathrm{e}^{-k_c \frac{|X_0|}{\varepsilon^2}} \mathrm{e}^{\mathrm{i}\omega},
\end{aligned} \tag{31}$$

and for $\hat{\theta} = 0$ the exponential small factor can thus be canceled. Indeed the error R_N^T, as derived below, is of the form $\tilde{S}_0(X)\mathrm{e}^{\mathrm{i}k_c x} + \text{c.c.} + O(\varepsilon)$, i.e. we have to rewrite $\mathrm{e}^{\mathrm{i}k_c x}$ in terms of X for the contribution of p_1, but $\mathrm{e}^{-\mathrm{i}k_c x}$ for the contribution of p_2. Thus the exponential smallness is only canceled for p_1 and the contribution of p_2 is not of leading order. In summary, for $\theta \approx 0$ and λ_δ sufficient small the error by truncation is dominant, while for $|\theta| \gg 0$ the error derived in section 4.2 is dominant, and a matching of both terms will yield the condition for localized

pattern. This matching will be made possible with the multi scales ansatz

$$R_N^T = \varepsilon^{-2\alpha}\left(R_N(x,\hat\theta) + \varepsilon R_{N+1}(x,\hat\theta) + \varepsilon^2 R_{N+2}(x,\hat\theta) + \dots\right)$$

in x and $\hat\theta$. To keep the notation simple and as we do not need the abstract form of the expansions terms outside of this paragraph we named them $R_N, R_{N+1}, \dots$ again, even though this is ambivalent with our notation for the whole error term. We can treat r as constant here, as derivatives of r do not occur in leading order. As we seek for the dependence of $\partial_{\hat\theta}$, we have to rewrite ∂_X in terms of this, i.e.

$$\partial_X = (\partial_\theta X)\partial_\theta = \frac{-\mathrm{i}}{r}\mathrm{e}^{-\mathrm{i}\theta}\partial_\theta = \frac{\mathrm{e}^{-\mathrm{i}\varepsilon\hat\theta}}{\varepsilon r}\partial_{\hat\theta} = \frac{1-\mathrm{i}\varepsilon\hat\theta-\varepsilon^2\hat\theta+\dots}{\varepsilon r}\partial_{\hat\theta},$$
$$\partial_X^2 = \left(\frac{\mathrm{e}^{-\mathrm{i}\varepsilon\hat\theta}}{\varepsilon r}\partial_{\hat\theta}\right)^2 = \frac{\mathrm{e}^{-\mathrm{i}\varepsilon\hat\theta}}{\varepsilon r}\left(\frac{\mathrm{e}^{-\mathrm{i}\varepsilon\hat\theta}}{\varepsilon r}\partial_{\hat\theta}^2 - \mathrm{i}\frac{\mathrm{e}^{-i\varepsilon\hat\theta}}{r}\partial_{\hat\theta}\right) = \frac{1}{\varepsilon^2 r^2}\partial_{\hat\theta}^2 + O\left(\frac{1}{\varepsilon}\right).$$

Next we sort (26) for powers of ε. For this we rewrite the leading order inhomogeneity (27) as $\varepsilon T_1 + \varepsilon^2 T_2 + O(\varepsilon^3)$, where the scaling is given by (29) and (30), to obtain

$$\begin{aligned}
\varepsilon^0:\ & 0 = \left(J(\lambda_c) + \partial_x^2 D\right) R_N\\
\varepsilon^1:\ & T_1 = \left(J(\lambda_c) + \partial_x^2 D\right) R_{N+1} + \frac{2}{r} D\partial_x\partial_{\hat\theta} R_{N+1} + 2F_0^2[\lambda_c,\sigma_0](U_1,R_N)\\
\varepsilon^2:\ & T_2 = \left(J(\lambda_c) + \partial_x^2 D\right) R_{N+2} + \frac{2}{r} D\partial_x\partial_{\hat\theta} R_{N+1} + 2F_0^2[\lambda_c,\sigma_0](U_1,R_{N+1})\\
& \quad - \mathrm{i}2\frac{\hat\theta}{r} D\partial_x\partial_{\hat\theta} R_N + \frac{1}{r^2} D\partial_{\hat\theta}^2 R_N + 2F_0^2[\lambda_c,\sigma_0](U_2,R_N) + 3F_0^3[\lambda_c,\sigma_0](U_1,U_1,R_N). \quad (32)
\end{aligned}$$

At ε^0 this yields $R_N = S_0\Phi e_1 + \hat S_0\Phi e_{-1}$, while T_1, T_2 are nonzero at e_0, e_2 only, and thus we need to express the factor $\mathrm{e}^{\mathrm{i}k_c x}$ in U through X, as done in (31). T_1, T_2 are calculated by (27), (29), (30), (31) and we have

$$\begin{aligned}
T_1 &= -p_1 2\sqrt{2\pi}\mathrm{i}^{-\alpha}k_c^\alpha (k_c r)^{-\frac{1}{2}}\mathrm{e}^{-\frac{k_c r}{\varepsilon^2}}\mathrm{e}^{-\mathrm{i}\varepsilon\hat\theta\left(\frac{k_c r}{\varepsilon^2}-1\right)}k_c^2\mathrm{e}^{k_c\frac{r\mathrm{e}^{\mathrm{i}\varepsilon\hat\theta}}{\varepsilon^2}}\mathrm{e}^{\mathrm{i}k_c\frac{x_0}{\varepsilon^2}}\mathrm{e}^{\mathrm{i}\omega}\left(2I_2 e_{-1} - 2I_1 e_1\right) D\Phi,\\
T_2 &= 2p_1\sqrt{2\pi}\mathrm{i}^{-\alpha}k_c^\alpha (k_c r)^{-\frac{1}{2}}\mathrm{e}^{-\frac{k_c r}{\varepsilon^2}}\mathrm{e}^{-\mathrm{i}\varepsilon\hat\theta\left(\frac{k_c r}{\varepsilon^2}-1\right)}k_c^2\hat\theta\mathrm{e}^{k_c\frac{r\mathrm{e}^{\mathrm{i}\varepsilon\hat\theta}}{\varepsilon^2}}\mathrm{e}^{\mathrm{i}k_c\frac{x_0}{\varepsilon^2}}\mathrm{e}^{\mathrm{i}\omega}\left(3I_2 e_{-1} - 1I_1 e_1\right) D\Phi.
\end{aligned}$$

As $T_1, T_2 \in \mathrm{span}\,(D\Phi)$, i.e. $\langle T_1, \Phi_\perp\rangle = \langle T_2, \Phi_\perp\rangle = 0$, there is no solvability condition at ε^1, and T_2 does not occur in the solvability condition at ε^2, i.e. in the calculation of S_0. Also note that (10) holds and thus

$$2F_0^2[\lambda_c,\sigma_0](U_2,R_N) + 3F_0^3[\lambda_c,\sigma_0](U_1,U_1,R_N)\big|_{e_{\pm1}} = -2F_0^2[\lambda_c,\sigma_0](U_1,\tilde R_{N+1})\big|_{e_{\pm1}},$$

where $\tilde R_{N+1}$ denotes the $e_0, e_{\pm2}$ parts of R_{N+1}. In summary (32) is solvable if and only if

$$0 = \left(J(\lambda_c) + \partial_x^2 D\right) R_{N+2} + \frac{2}{r} D\partial_x\partial_{\hat\theta} R_{N+1} - \mathrm{i}2\frac{\hat\theta}{r} D\partial_x\partial_{\hat\theta} R_N + \frac{1}{r^2}\partial_{\hat\theta}^2 D R_N,$$

which itself is solvable if and only if

$$0 = \left\langle \frac{2}{r} D\partial_x\partial_{\hat\theta} R_{N+1}\Big|_{e_{\pm1}}, \Phi_\perp \right\rangle, \quad (33)$$

as again $\langle D\Phi, \Phi_\perp\rangle = 0$. To solve (33) we need the orthogonal projection of $R_{N+1}|_{e\pm 1}$ onto span $\{\Phi\}^\perp$, which is

$$\left(\frac{i}{r}\partial_{\hat\theta}S_0 + \left.\frac{\langle T_1, D\Phi\rangle}{2k_c\|D\Phi\|}\right|_{e_1}\right)\Phi_{3,1}e_1 + \text{c.c.}.$$

Thus the equation for S_0 is

$$\begin{aligned}0 &= \left(-k_c\frac{2}{r^2}\partial_{\hat\theta}^2 S_0 + \mathrm{i}k_c\frac{2}{r}\partial_{\hat\theta}\left.\frac{\langle T_1, D\Phi\rangle}{2k_c\|D\Phi\|}\right|_{e_1}\right)\langle D\Phi_{3,1}, \Phi_\perp\rangle\,.\\ \Leftrightarrow \partial_{\hat\theta}^2 S_0 &= \mathrm{i}r\partial_{\hat\theta}\left.\frac{\langle T_1, D\Phi\rangle}{2k_c\|D\Phi\|}\right|_{e_1}.\end{aligned}$$

Obviously S_0 can be calculated by integrating twice, but before that we derive the $\hat\theta$ dependence of $r\frac{\langle T_1, D\Phi\rangle}{2k_c\|D\Phi\|}$ at e_1:

$$\begin{aligned}r\left.\frac{\langle T_1, D\Phi\rangle}{2k_c\|D\Phi\|}\right|_{e_1} &= -\mathrm{i}p_1\sqrt{2\pi}i^{-\alpha}k_c^\alpha(k_cr)^{\frac12}\mathrm{e}^{-\frac{k_cr}{\varepsilon^2}}\mathrm{e}^{-\mathrm{i}\varepsilon\hat\theta\left(\frac{k_cr}{\varepsilon^2}-1\right)}\mathrm{e}^{k_c\frac{re^{\mathrm{i}\varepsilon\hat\theta}}{\varepsilon^2}}\mathrm{e}^{\mathrm{i}k_c\frac{X_0}{\varepsilon^2}}2\mathrm{e}^{\mathrm{i}\omega}I_1(X)e_1\\ &= -p_1\sqrt{2\pi}\mathrm{i}^{1-\alpha}k_c^{\alpha+\frac12}r^{\frac12}\mathrm{e}^{-\frac{k_cr}{\varepsilon^2}}\mathrm{e}^{-\mathrm{i}\varepsilon\hat\theta\left(\frac{k_cr}{\varepsilon^2}-1\right)}\mathrm{e}^{\frac{k_cr}{\varepsilon^2}\left(1+\mathrm{i}\varepsilon\hat\theta-\varepsilon^2\hat\theta^2+O(\varepsilon^3)\right)}\mathrm{e}^{\mathrm{i}k_c\frac{X_0}{\varepsilon^2}}2\mathrm{e}^{\mathrm{i}\omega}I_1(X)e_1\\ &\underset{\varepsilon\to0}{\sim} -p_1\sqrt{2\pi}\mathrm{i}^{1-\alpha}k_c^{\alpha+\frac12}r^{\frac12}\mathrm{e}^{\frac{k_cr}{\varepsilon^2}\left(-\varepsilon^2\hat\theta^2\right)}\mathrm{e}^{\mathrm{i}k_c\frac{X_0}{\varepsilon^2}}2\mathrm{e}^{\mathrm{i}\omega}I_1(X_0-\mathrm{i}r)e_1\\ &= -p_12\sqrt{2\pi}\mathrm{i}^{1-\alpha}k_c^{\alpha+\frac12}r^{\frac12}\mathrm{e}^{-k_cr\hat\theta^2}\mathrm{e}^{\mathrm{i}k_c\frac{X_0}{\varepsilon^2}}\mathrm{e}^{\mathrm{i}\omega}I_1(X_0-\mathrm{i}r)e_1,\end{aligned}\tag{34}$$

where $I_{1,2}(X) = I_{1,2}(X_0 - \mathrm{i}r) + O(\varepsilon)$ by the Taylor series in $\hat\theta$, as $X = X_0 - re^{\mathrm{i}\varepsilon\hat\theta}$. This then finally yields

$$\begin{aligned}S_0 &= -p_12\sqrt{2\pi}\mathrm{i}^{1-\alpha}k_c^{\alpha+\frac12}r^{\frac12}\mathrm{e}^{\mathrm{i}k_c\frac{X_0}{\varepsilon^2}}\mathrm{e}^{\mathrm{i}\omega}I_1(X_0-\mathrm{i}r)\left(\int_0^{\hat\theta}\mathrm{e}^{-k_crx^2}\mathrm{d}x + C_1\right)\\ &= -p_1\pi\sqrt{2}\mathrm{i}^{1-\alpha}k_c^\alpha\mathrm{e}^{\mathrm{i}k_c\frac{X_0}{\varepsilon^2}}\mathrm{e}^{\mathrm{i}\omega}I_1(X_0-\mathrm{i}r)\left(\operatorname{erf}(\sqrt{k_cr}\hat\theta) + C_1\right),\end{aligned}$$

with constants C_1, C_{-1} and where we set the first constant of integration to zero, as we always seek a bounded solution. At $\varepsilon^2 e_{-1}$ a solvability condition for $\hat S_0$ arises in exactly the same matter and yields $\hat S_0 = -\bar S_0$.

Now recall that we simplified the calculation by ignoring the c.c. in U_n, and thus for the real S_0 we have to add that again. As mentioned above, the linearity of the calculations yields that we just have to add the complex conjugate, i.e. the full solution at e_1 is given by $S_0 + \bar S_0$, and as $I_1 = \bar I_2$ for real X, see theorem 4.1, the full contribution at e_1 on the real line is given by

$$\begin{aligned}&\Im\left(-p_1\pi\sqrt{2}\mathrm{i}^{1-\alpha}k_c^\alpha\mathrm{e}^{\mathrm{i}k_c\frac{X_0}{\varepsilon^2}}\mathrm{e}^{\mathrm{i}\omega}\right)I_1(X_0-\mathrm{i}r)\left(\operatorname{erf}(\sqrt{k_cr}\hat\theta) + (C_1+\bar C_{-1})\right)\\ &= -\pi\sqrt{2}\varepsilon^{-6}|p_1|k_c^{\frac52}\mathrm{e}^{\mathrm{i}k_c\frac{X_0}{\varepsilon^2}}\mathrm{e}^{-\frac12\pi\beta}I_1(X_0-\mathrm{i}r)\\ &\quad\sin(\ln(k_c)\beta + \arg(p_1) - 2ln(\varepsilon)\beta + \omega)\left(\operatorname{erf}(\sqrt{k_cr}\hat\theta) + (C_1+\bar C_{-1})\right),\end{aligned}\tag{35}$$

as $\alpha = 3 + \mathrm{i}\beta$. Remember that ω was the arbitrary phase shift in the leading order, which we reintroduced here, because it is crucial for the upcoming matching process. □

4.4. Matching of the remainder terms and the snaking width formula

The leading order forcing by truncation, calculated in (34), is exponential decaying in $\hat{\theta}$. As $X - X_0 = -\mathrm{i}r\mathrm{e}^{\mathrm{i}\varepsilon\hat{\theta}}$ the forcing by truncation thus is relevant in an $X = O(\varepsilon)$ range, the Stokes layer, only. Thus the error of truncation is the leading order error outside of the Stokes layer, and both errors have to match at this border.

The matching progress leads to the following theorem, from which theorem 2.4 is a direct corollary, and thus yields our main result.

Theorem 4.5. *Let (5) be an asymptotic expansion of a front solution U_ε^f as in hypothesis 2.2. Then the leading order remainder $R_N^T + \varepsilon R^{\lambda_\delta}$ is uniformly exponentially small in $\varepsilon^2\sigma_2 = \sigma - \sigma_0$ if and only if*

$$|\lambda - \lambda_\mathrm{M}| = \left|\varepsilon^4\lambda_\delta\right| < \frac{\mu}{|\sigma - \sigma_0|}\mathrm{e}^{-\frac{\nu}{|\sigma-\sigma_0|}} \tag{36}$$

where $\nu \approx 18.550\frac{1}{\sqrt{d}}$ and $\sigma_0 \approx -2.4\sqrt{d}$ in case 1, while $\nu \approx 69.721\frac{1}{\sqrt{d}}$ and $\sigma_0 \approx -16\sqrt{d}$ in case 2.

The linear nature of the method makes it unable to determine μ, which will thus be determined by a numerical fit in section 6. Indeed (18) can be used to establish μ via an recurrent limit, but it is cumbersome to approximate this limit, see [DMCK11], why we omit this step here.

Proof. Now that we found the error by truncation R_N^T and the Maxwell point deviation error R^{λ_δ} we can match both at the Stokes layer borders, i.e. for $\hat{\theta} = O(\frac{1}{\varepsilon})$. Afterwards we investigate the remainder in the limit $X \to \infty$ and derive conditions for uniform exponential smallness. In section 4.2 we showed

$$R_{1,1}^{\lambda_\delta} = K_3 I_1 + \left(\frac{2\sqrt{15}}{c_0}\lambda_\delta R_0' \int \frac{R_0^2}{R_0'^2} + i2\hat{c}\frac{2\sqrt{15}}{c_0}\lambda_\delta R_0 \int R_0 R_0' \int \frac{R_0^2}{R_0'^2}\right)\mathrm{e}^{\mathrm{i}\Theta_0} =: K_3 I_1 + \lambda_\delta I_{\lambda_\delta}, \tag{37}$$

where we already set the constants K_1, K_2 and K_4 to zero, as a nonzero factor K_1 would yield an unbounded solution and nonzero factors K_2 or K_4 correspond to infinitesimal translations in X resp. x. As $I_1 \to \infty$ and $I_{\lambda_\delta} \to 0$ for $X \to -\infty$ we have $K_3 = 0$ for $X < 0$. Furthermore $I_{\lambda_\delta}(0) = 0$ and $S_0 \to \text{const.} \cdot \left(C_1 + \bar{C}_{-1} - 1\right)$ for $\hat{\theta} \to -\infty$ which yields $C_1 + \bar{C}_{-1} = 1$ to match at the left hand side of the Stokes layer.

At the right hand side of the Stokes layer we thus require

$$K_3 = -\varepsilon^{-5} 4|p_1|\sqrt{2}k_c^3 \mathrm{e}^{\mathrm{i}k_c\frac{X_0}{\varepsilon^2}}\mathrm{e}^{-\frac{1}{2}\pi\beta}\sin(\ln(k_c)\beta - 2\ln(\varepsilon)\beta + \arg(p_1) + \omega),$$

to match S_0, see (35) with (37). The missing ε factor is due to our scaling $R_N^T + \varepsilon R^{\lambda_\delta}$ for the leading order remainder. Continuity is recovered by adding both error terms and subtracting matched parts. For conditions on λ_δ we only need to investigate the limit $X \to \infty$ where $I_1, I_{\lambda_\delta} \to \infty$. Therefore, recall that

$$I_1 = \left(R_0' \int_{X_0}^{X} \frac{1}{R_0'^2} \mathrm{d}t + \mathrm{i}2\hat{c} R_0 \int_{X_0}^{X} R_0 R_0' \int_{X_0}^{s} \frac{1}{R_0'^2} \mathrm{d}t \mathrm{d}s \right) \mathrm{e}^{\mathrm{i}\Theta_0} \quad \text{and} \quad R_0 = \frac{b_1}{\sqrt{1+\mathrm{e}^{b_2 X}}}$$

with $b_2 < 0 < b_1$ from theorem 3.1. For $X \to \infty$ we have

$$R_0 \underset{X\to\infty}{\sim} b_1 \left(1 - \frac{\mathrm{e}^{b_2 X}}{2}\right)$$

and thus

$$I_1 \underset{X\to\infty}{\sim} \left(\frac{1}{b_1 b_2^2} \mathrm{e}^{-b_2 X} - \mathrm{i}2\hat{c} \frac{b_1}{b_2^3} \mathrm{e}^{-b_2 X} \right) \mathrm{e}^{\mathrm{i}\Theta_0} = \frac{1}{b_1 b_2^2} \left(1 - \mathrm{i}2\hat{c} \frac{b_1^2}{b_2}\right) \mathrm{e}^{\mathrm{i}\Theta_0} \mathrm{e}^{-b_2 X},$$

and

$$\frac{2\sqrt{15}}{c_0} \lambda_\delta \left(R_0' \int_0^X \frac{R_0^2}{R_0'^2} \mathrm{d}T + \mathrm{i}2\hat{c} R_0 \int_0^X R_0 R_0' \int_{X_0}^X \frac{R_0^2}{R_0'^2} \right) \mathrm{e}^{\mathrm{i}\Theta_0} \underset{X\to\infty}{\sim} \frac{2\sqrt{15}}{c_0} \lambda_\delta \frac{b_1}{b_2^2} \left(1 - \mathrm{i}2\hat{c} \frac{b_1^2}{b_2}\right) \mathrm{e}^{\mathrm{i}\Theta_0} \mathrm{e}^{-b_2 X}.$$

This yields the exponentially growing term

$$\begin{aligned} &\left(-\varepsilon^{-6} \pi |p_1| \sqrt{2} k_c^3 \mathrm{e}^{\mathrm{i}k_c \frac{X_0}{\varepsilon^2}} \mathrm{e}^{-\frac{1}{2}\pi\beta} \sin(\ln(k_c)\beta - 2\ln(\varepsilon)\beta + \arg(p_1) + \omega) \right. \\ &\left. \frac{1}{b_1 b_2^2} + \frac{2\sqrt{15}}{c_0} \lambda_\delta \frac{b_1}{b_2^2} \right) \left(1 - \mathrm{i}2\hat{c} \frac{b_1^2}{b_2}\right) \mathrm{e}^{\mathrm{i}\Theta_0} \mathrm{e}^{-b_2 X}. \end{aligned} \tag{38}$$

Thus, there is only a small range of λ_δ for which we can find ω to cancel the exponential factor, i.e. where we have a uniform exponentially small remainder and thus a front. The precise range for case 1 is

$$\begin{aligned} |\lambda_\delta| &\leqslant \frac{\varepsilon^{-6} \pi |p_1| \sqrt{2} k_c^3 \mathrm{e}^{\mathrm{i}k_c \frac{X_0}{\varepsilon^2}} \mathrm{e}^{-\frac{1}{2}\pi\beta}}{b_1 b_2^2 \frac{2\sqrt{15}}{c_0} \frac{b_1}{b_2^2}} = \frac{\text{const.}}{\varepsilon^4} \frac{1}{\varepsilon^{-2} b_1^2} \mathrm{e}^{\mathrm{i}k_c \frac{X_0}{\varepsilon^2}} \\ &= \frac{\text{const.}}{\varepsilon^4} \frac{1}{|\sigma - \sigma_0|} \mathrm{e}^{-k_c \frac{|X_0|}{\varepsilon^2}} \approx \frac{\text{const.}}{\varepsilon^4 |\sigma - \sigma_0|} \mathrm{e}^{-\frac{18.550}{\sqrt{d}|\sigma - \sigma_0|}}. \end{aligned}$$

Importantly, most constants in the exponential decay, namely X_0 and k_c are determined directly by the leading order solution A and thus can be calculated without the heavy computations of the beyond all order methods, as already noted in the introduction. Besides justification the beyond all order calculations also yield the dominant wavenumbers in U_n for $n \to \infty$, which results in an integer factor in the exponential decay (which is 1 here), and is determined by the lowest order nonlinearity in the underlying model, i.e. can be guessed without the calculations as well. □

5. Construction of the snakes

The Schnakenberg model is local and invariant under translation and the symmetry $x \to -x$, which together implies that the existence of fronts is in a one to one correspondence to the

existence of localized patterns with sufficient width. Still the actual gluing of two fronts to form a localized pattern yields some additional insights. We therefore give a brief summary of this method and discuss its consequences for the snaking branch. This is not formulated in a theorem, as we skip some details and thus do not derive the gluing rigorously.

A localized pattern, constructed by the gluing of two fronts, is—for a sufficient pattern length—approximated well by front solutions at the borders, and a matching of these gives the existence range and the asymptotics of the snaking branch for $\sigma \to \sigma_0$. By (38) the remainder has the two exponential terms $\mathrm{e}^{-\mathrm{i}k_c \frac{X_0}{\varepsilon^2}}$ and $\mathrm{e}^{-b_2 X}$. As $X_0 = \mathrm{i}\pi/k_c$, exponential growing terms are switched on for $X = O\left(\frac{1}{\varepsilon^2}\right)$. Thus a matching of an up- and down-front is possible, i.e. growing terms are of the same size, if the patterns length is $O\left(\frac{1}{\varepsilon^4}\right)$. We denote the patterns length by L/ε^4, $L \in \mathbb{R}$.

An asymptotic expansion for the up-front was constructed in the previous sections. By the reflection $(x, X) \to (-x, -X)$ we have a down-front solution as well. To construct a localized pattern $p(x, X)$ centered at $L/2\varepsilon^4$ we shift the down-front by L/ε^4. For $1 \ll X \ll 1/\varepsilon^2$ we can approximate p by $\varepsilon U_1 + R_N$ and simplify this in the limit $X \to \infty$, as we match at $X = O\left(\frac{1}{\varepsilon^2}\right)$. Precisely we have

$$p(x,X) \underset{X\to\infty}{\sim} b_1 \mathrm{e}^{\mathrm{i}b_2\beta X}\mathrm{e}^{\mathrm{i}k_c(x+\omega)}\left(1 - \left(\frac{1}{2} + \mathrm{i}\beta\right)\mathrm{e}^{b_2 X} + (1 - \mathrm{i}2\beta)\frac{1}{b_2}\Xi(\omega)\mathrm{e}^{-b_2 X}\right) + \text{c.c.} \tag{39}$$

with

$$\Xi(\omega) = \left(-\varepsilon^{-6}\pi|p_1|\sqrt{2}k_c^3 \mathrm{e}^{\mathrm{i}k_c\frac{X_0}{\varepsilon^2}}\mathrm{e}^{-\frac{1}{2}\pi\beta}\sin(\ln(k_c)\beta - 2\ln(\varepsilon)\beta + \arg(p_1) + \omega)\frac{1}{b_1 b_2^2} + \frac{2\sqrt{15}}{c_0}\lambda_\delta\frac{b_1}{b_2^2}\right).$$

This approximates p at the left border of the pattern, i.e. the up-front. By symmetry the right border, i.e. the down-front, is approximated well for $1 \ll L/\varepsilon^2 - X \ll 1/\varepsilon^2$ by

$$\begin{aligned} p(x,X) &\underset{X\to\infty}{\sim} b_1 \mathrm{e}^{\mathrm{i}b_2\beta\left(\frac{L}{\varepsilon^2}-X\right)}\mathrm{e}^{\mathrm{i}k_c\left(\left(\frac{L}{\varepsilon^4}-x\right)+\hat{\omega}\right)}\left(1 - \left(\frac{1}{2} + \mathrm{i}\beta\right)\mathrm{e}^{b_2\left(\frac{L}{\varepsilon^2}-X\right)} + (1 - \mathrm{i}2\beta)\frac{1}{b_2}\Xi(\hat{\omega})\mathrm{e}^{-b_2\left(\frac{L}{\varepsilon^2}-X\right)}\right) + \text{c.c.} \\ &= b_1 \mathrm{e}^{-\mathrm{i}b_2\beta\left(\frac{L}{\varepsilon^2}-X\right)}\mathrm{e}^{-\mathrm{i}k_c\left(\left(\frac{L}{\varepsilon^4}-x\right)+\hat{\omega}\right)}\left(1 - \left(\frac{1}{2} - \mathrm{i}\beta\right)\mathrm{e}^{b_2\left(\frac{L}{\varepsilon^2}-X\right)} + (1 + \mathrm{i}2\beta)\frac{1}{b_2}\Xi(\hat{\omega})\mathrm{e}^{-b_2\left(\frac{L}{\varepsilon^2}-X\right)}\right) + \text{c.c.} \end{aligned} \tag{40}$$

where we introduced $\hat{\omega}$ as the phase-shift of the down-front, because both fronts are not enforced to have the same phase-shift, and indeed we find precise matching conditions between both phase shifts for different snaking branches.

Following [CK09], a substantially better approximation would be given by $p \sim \varepsilon U_1 + \varepsilon^2 U_2 + R_N$ in the up-front region and similarly in the down-front region, because U_2 yields the term $C = \varepsilon^2 X \mathrm{e}^{b_2 X}$, and $\varepsilon^2 X = O(1)$ in the matching regime $X = O\left(\frac{1}{\varepsilon^2}\right)$, i.e. C has to be included in the matching process. This would then stop the approximations (39) and (40) from being uniformly valid at $X = O\left(\frac{1}{\varepsilon^2}\right)$ and therefore require to recalculate the asymptotic expansion of the front with a super slow scale $\xi = \varepsilon^4 x$. Additionally, one would need to derive a series for the periodic solution itself and treat the fronts as borders. But, as the amplitude to the periodic solution can, in view of (39), be expected to be a constant plus an exponential small correction in X, i.e. to be of the form

$$b_1 \mathrm{e}^{-\mathrm{i}b_2\beta X}\mathrm{e}^{\mathrm{i}k_c\left(x+\hat{\omega}\right)}\left(a_0 + a_\pm \mathrm{e}^{\pm(b_2 X + \gamma\psi)}\right) + \text{c.c.}$$

with constants $a_0, a_\pm$ and γ, this would result in negligible corrections only.

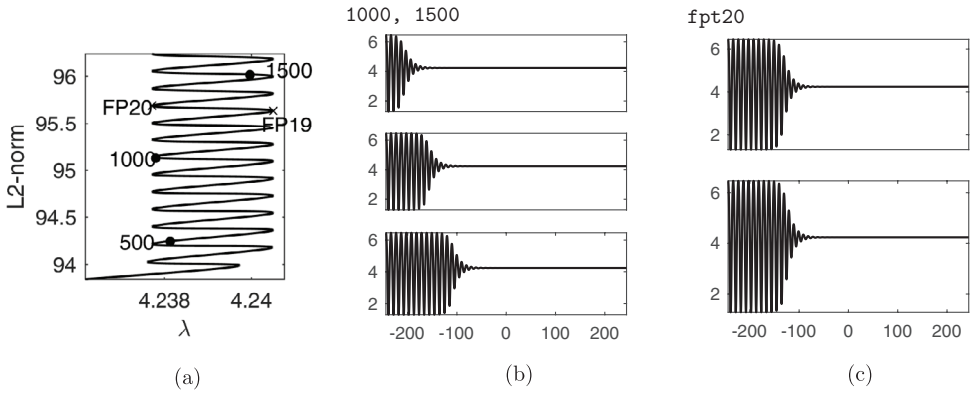

Figure 3. (a) Excerpt of the numerical snaking branch of localized patterns for the truncated system (7) with $d = 100$ and $\sigma = -0.5$. Stability is not plotted for clarity; computations show that every second winding is stable. (b) Some solution plots on the snake. Only the first component of $U = (u, v)$ is shown. (c) As (b) for the fold points, which are continued to compute the snaking width. The parameter $\sigma = -0.5$ is far away from the range where our method is expected to give good results, which is also indicated by the $O(1)$ amplitudes of the solutions and was chosen for visual reasons, as even here the snaking width is of magnitude 10^{-3} only, also see figure 4.

The matching itself is done by equating like terms in (39) and (40). The constant terms in X yield

$$\omega = b_2\beta\frac{L}{\varepsilon^2} - k_c\frac{L}{\varepsilon^4} - \hat{\omega} + 2\pi\mathbb{Z}. \tag{41}$$

Equating the exponential terms then yields

$$\frac{1}{2} = \frac{1}{b_1}\Xi(\hat{\omega})\mathrm{e}^{-b_2\frac{L}{\varepsilon^2}},\ \frac{1}{b_1}\Xi(\omega) = \frac{1}{2}\mathrm{e}^{b_2\frac{L}{\varepsilon^2}}.$$

Thus $\Xi(\omega) = \Xi(\hat{\omega})$ is required. This has the two solution branches

Case 1: $\omega = \hat{\omega} + 2\pi\mathbb{Z}$,
Case 2: $\omega = -\hat{\omega} + \pi - 2\left(\ln(k_c)\beta - 2\ln(\varepsilon)\beta + \arg(p_1)\right) + 2\pi\mathbb{Z}$,

and requires

$$\frac{b_1}{2}\mathrm{e}^{b_2\frac{L}{\varepsilon^2}} = \varepsilon^{-4}\tilde{p}_1\mathrm{e}^{-\frac{k_c\pi}{b_2\varepsilon^2}}\sin(p_2 - 2\beta\ln(\varepsilon) + \omega) + \lambda_\delta, \tag{42}$$

where $\tilde{p}_1(|\sigma - \sigma_0|)$ and p_2 now condense the angular respectively absolute value of the numerically determined constant p_1 along with some further constants for clarity.

Suppose that case 1 holds now. Then

$$\omega = \frac{b_2\beta}{2}\frac{L}{\varepsilon^2} - \frac{k_c}{2}\frac{L}{\varepsilon^4} + \pi\mathbb{Z}$$

by (41) and thus (42) yields

$$\lambda_\delta = \frac{b_1}{2}\mathrm{e}^{b_2\frac{L}{\varepsilon^2}} - \varepsilon^{-4}\tilde{p}_1\mathrm{e}^{-\frac{k_c\pi}{b_2\varepsilon^2}}\sin(p_2 - 2\beta\ln(\varepsilon) + \frac{b_2\beta}{2}\frac{L}{\varepsilon^2} - \frac{k_c}{2}\frac{L}{\varepsilon^4} + k\pi) \tag{43}$$

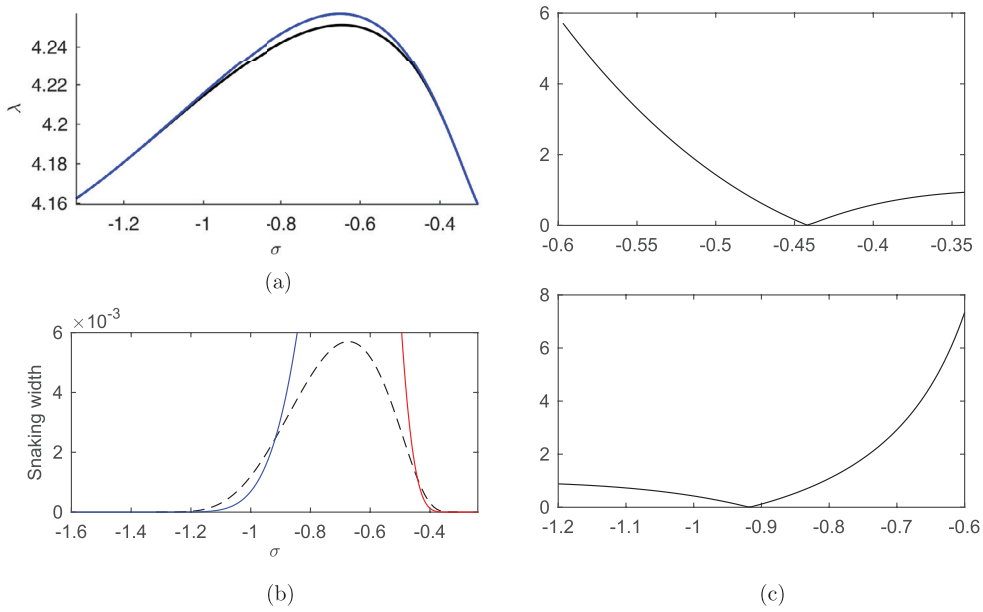

Figure 4. (a) Fold point continuation of `fpt19` (blue) and `fpt20` (black) in σ. (b) Numerically estimated snaking width (black) and analytical predictions (blue, red lines) with a best fit for μ. Numerical snaking widths in the regimes $\sigma < -1.2$ and $\sigma > -0.342$ have not been taken into account, as the computed widths are below numerical resolution. (c) Relative errors with regard to the numerical estimate of the snaking width, where the turning point for the range of localized patterns is roughly at $\sigma = -0.6$.

with $k \in \{0, 1\}$. This corresponds to the two snaking curves, one with a maximum at the patterns center and one with a minimum. As $b_2 < 0$ the term $\frac{b_1}{2} e^{b_2 \frac{L}{\varepsilon^2}}$ is negligible for $L \gg k_c \pi$ and (42) transforms into the formula for the width of existence again. Additionally one can observe in (43) that a change of L by $4\pi\varepsilon^4/k_c$ roughly, i.e. in leading order, implies the snake to go up one turn. More precise, as $b_2 \approx 0.029\sqrt{d}\sigma_2 = \frac{1}{\varepsilon^2} 0.029\sqrt{d}\,(\sigma - \sigma_0)$ the increase of L by $4\pi\varepsilon^4 / \left(k_c + 0.029\sqrt{d}\,|\sigma_2 - \sigma_0|\,\beta\right)$ will give the snake another turn and corresponds to two bumbs being added to the pattern, as the wavenumber is manipulated by the complex amplitude.

If case 2 holds, (41) fixes L while ω stays arbitrary and thus for all λ_δ in an exponentially small range one can find ω to solve (42). For large L one can again ignore the $e^{-b_2 \frac{L}{\varepsilon^2}}$ factor and see that this case describes the ladders, horizontal branches of asymmetric solutions connecting the two snaking curves close to their fold points. However, these are expected to slowly travel in time in non-variational systems, see e.g. [BD12, BKL$^+$09, BK07], which is an effect on an even slower scale, and thus ladders can not be observed in this system.

6. Numerics and comparison with the analysis

The numerical results for all calculations are computed with pde2path [URW14] on the interval $I = \left(-25\frac{2\pi}{k_c}, 25\frac{2\pi}{k_c}\right)$ with Neumann boundary conditions. For plots the domain is sometimes reduced, but for computations like the fit of μ the domain I is used. Front solutions

on this domain with interface size smaller than 50 periods can then, by mirroring and gluing together, be identified with localized patterns on the real line. While boundary effects for localized patterns are rapidly decreasing the huge domain size is necessary to track localized patterns for $|\sigma - \sigma_0|$ small, because the slow scale of the interface yields a very large interface section. The diffusion parameter d was set to 100, as there is a trade-off between the existence range of localized patterns and thus non-linear forcing on the snaking width and the number of unstable wavelengths for $\lambda = \lambda_c + O\left(\varepsilon^4\right)$, which makes the numerics somewhat delicate. Another difficulty for small d is the high exponential forcing, which scales with $d^{-\frac{1}{2}}$, see theorem 4.5, and results in snaking widths below numerical resolution for $\sigma - \sigma_0 = O(1)$.

We present the numerics for the truncated system (7) as it contains every information used in our analysis. Figure 3 shows the snaking branch of localized patterns for $\sigma = 0.5$ along with some solutions on that branch. The fold points `fpt19` and `fpt20` are tracked by a fold continuation in σ, which results in figure 4(a), and the snaking width is determined by the difference of both fold positions. The numerical snaking width and the analytical estimate are shown in figure 4(b), where μ is chosen as a best fit in the regime, where the differential of the numerical snaking width increases, respectively decreases. The calculations show that, even though the snaking width differs from our estimate, the relative error is small for width variations of order 10^4.

Similar results are obtained for the full system, with different μ, which incorporates the higher order nonlinearities, and we omit plots for the sake of brevity.

Acknowledgments

I am grateful to H Uecker and D Wetzel for enlightening discussions and helpful comments.

References

[BD12] Burke J and Dawes J H P 2012 Localized states in an extended Swift–Hohenberg equation *SIAM J. Appl. Dyn. Syst.* **11** 261–84

[BK07] Burke D and Knobloch E 2007 Homoclinic snaking: structure and stability *Chaos* **17** 037102

[BKL+09] Beck M, Knobloch J, Lloyd D J B, Sandstede B and Wagenknecht T 2009 Snakes, ladders, and isolas of localized patterns *SIAM J. Math. Anal.* **41** 936–72

[CK09] Chapman S J and Kozyreff G 2009 Exponential asymptotics of localised patterns and snaking bifurcation diagrams *Physica* D **238** 319–54

[Daw10] Dawes J H P 2010 The emergence of a coherent structure for coherent structures: localized states in nonlinear systems *Phil. Trans. R. Soc.* A **368** 3519–34

[Des11] Descalzi O 2011 *Localized States in Physics: Solitons and Patterns* (Berlin: Springer)

[DMCK11] Dean A D, Matthews P C, Cox S M and King J R 2011 Exponential asymptotics of homoclinic snaking *Nonlinearity* **24** 3323–51

[GT85] Goodwin B C and Trainor L E H 1985 Tip and whorl morphogenesis in acetabularia by calcium-regulated strain fields *J. Theor. Biol.* **117** 79–106

[KC13] Kozyreff G and Chapman S J 2013 Analytical results for front pinning between an hexagonal pattern and a uniform state in pattern-formation systems *Phys. Rev. Lett.* **111** 054501

[Kno08] Knobloch E 2008 Spatially localized structures in dissipative systems: open problems *Nonlinearity* **21** T45

[Kno15] Knobloch E 2015 Spatial localization in dissipative systems *Annu. Rev. Condens. Matter Phys.* **6** 325–59

[Mur89] Murray J D 1989 *Mathematical Biology* (Berlin: Springer) (https://doi.org/10.1007/978-3-662-08539-4)

[MYG07] Meron E, Yizhaq H and Gilad E 2007 Localized structures in dryland vegetation: Forms and functions *Chaos* **17** 037109

[RAB+13] Rankin J, Avitabile D, Baladron J, Faye G and Lloyd D J B 2014 Continuation of localised coherent structures in nonlocal neural field equations *SIAM J. Sci. Comput.* **36** B70–B93

[Sch79] Schnakenberg J 1979 Simple chemical reaction systems with limit cycle behaviour *J. Theor. Biol.* **81** 389–400

[URW14] Uecker H, Rademacher J D M and Wetzel D 2014 pde2path - a Matlab package for continuation and bifurcation in 2D elliptic systems *Numer. Math.* **7** 58–106 (https://www.cambridge.org/core/journals/numerical-mathematics-theory-methods-and-applications/article/pde2path-a-matlab-package-for-continuation-and-bifurcation-in-2d-elliptic-systems/11B12FB6196D66ADCBE37A84944D7DC2)

[UW14] Uecker H and Wetzel D 2014 Numerical results for snaking of patterns over patterns in some 2D Selkov–Schnakenberg reaction–diffusion systems *SIADS* **13–1** 94–128